Temporal variability of suspended sediment sources in an alpine catchment combining river/rainfall monitoring and sediment fingerprinting

O. Navratil, O. Evrard, Michel Esteves, Cédric Legout, Sophie Ayrault, Julien Némery, Ainhoa Mate Marin, Mehdi Ahmadi, Irène Lefèvre, Alain Poirel, et al.

TEMPORAL VARIABILITY OF SUSPENDED SEDIMENT SOURCES IN AN ALPINE CATCHMENT COMBINING RIVER/RAINFALL MONITORING AND SEDIMENT FINGERPRINTING

Oldrich Navratil[a], Olivier Evrard[b], Michel Esteves[a], Cédric Legout[c], Sophie Ayrault[b], Julien Némery[d], Ainhoa Mate-Marin[a], Mehdi Ahmadi[b], Irène Lefèvre[a], Alain Poirel[e], Philippe Bonté[b]

[a] LTHE - Université Grenoble 1/IRD, BP 53, 38041-Grenoble Cedex 9 (France)

[b] Laboratoire des Sciences du Climat et de l'Environnement (LSCE/IPSL) – Unité Mixte de Recherche 8212 (CEA, CNRS, UVSQ), 91198-Gif-sur-Yvette Cedex (France)

[c] LTHE - Université Grenoble 1, BP 53, 38041-Grenoble Cedex 9 (France)

[d] LTHE - Université Grenoble 1/G-INP, BP 53, 38041-Grenoble Cedex 9 (France)

[e] EDF-DTG, Electricité de France, Grenoble Cedex 9 (France)

Correspondence to: Oldrich Navratil (navratiloldrich@gmail.com); Olivier Evrard (olivier.evrard@lsce.ipsl.fr)

Short title: Temporal variability of suspended sediment sources in mountains

Keywords: river gauging, suspended sediment fingerprinting, radar imagery, geochemistry, radionuclide, wash load

ABSTRACT

Influence of the rainfall regime on erosion and transfer of suspended sediment in a 905-km² mountainous catchment of the southern French Alps was investigated by combining sediment monitoring, rainfall data, and sediment fingerprinting (sediment geochemistry and radionuclide concentrations). Suspended sediment yields were monitored between October 2007 and December 2009 in four subcatchments (22−713 km²). Automatic sediment sampling was triggered during floods to trace the sediment origin in the catchment

Sediment exports at the river catchment outlet (330±100 t km^{-2} yr^{-1}) were mainly driven (80%) by widespread rainfall events (long duration, low intensities). In contrast, heavy, local and short duration storms, generated high peak discharges and suspended sediment concentrations in small upstream torrents. However, these upstream floods had generally not the capacity to transfer the sediment down to the catchment outlet and the bulk of this fine sediment deposited along downstream sections of the river. This study also confirmed the important contribution of black marls (up to 70%) to sediment transported in rivers, although this substrate only occupies ca. 10% of the total catchment surface. Sediment exports generated by local convective storms varied significantly at both intra- and inter-flood scales, because of spatial heterogeneity of rainfall. However, black marls/marly limestones contribution remained systematically high. In contrast, widespread flood events that generate the bulk of annual sediment supply at the outlet were characterised by a more stable lithologic composition and by a larger contribution of limestones/marls, Quaternary deposits and conglomerates, which corroborates the results of a previous sediment fingerprinting study conducted on riverbed sediment.

1. INTRODUCTION

Suspended sediment transported by rivers has fundamental environmental and economical consequences. An excess of sediment leads for instance to an increase in water turbidity, eutrophication, alteration of river habitats and reservoir siltation (e.g. Carpenter et al., 1998; Packman and Mackey, 2003; Owens et al., 2005). The suspended load comprises all the particles with a diameter lower than 2 mm (i.e. sand-sized or less). The finer particle fraction (<63 μm; i.e. silt and clay-sized material) transports a significant part of biogeochemical fluxes conveyed by rivers and its transfer needs to be better understood. By transporting the nutrients required by all the living organisms, fine sediment plays an essential role in the productivity of riverine, estuarine and marine ecosystems (House and Warwick, 1999; Collins et al., 2005). This fraction is also one of the main vectors of contaminants in rivers, including polychlorinated biphenyls (PCBs), dioxins, radionuclides, heavy and trace metals (Salomons and Forstner, 1984; Droppo, 2001; Walling and Collins, 2008). Very expensive management operations are generally achieved to cope with the problems associated with fine particle sedimentation. River dredging is often conducted to prevent flooding, to maintain navigation or to restore wetlands. Furthermore, the production of energy by hydroelectric power plants requires reliable predictions of Suspended Sediment Concentrations (SCC) and Yields (SSY) at the flood scale in order to avoid the major disturbances that could be induced by the massive and sudden siltation of reservoirs.

There is hence a preliminary need to evaluate the dynamics of suspended sediment within rivers in mountainous catchments in order to implement appropriate and effective control measures along the downstream river network. Suspended sediment supply to lowland rivers is indeed mainly dominated by local erosion processes and by the transfer of fine sediment from highly erodible mountainous catchments (Gallart et al., 2002; Regües and Gallart, 2004;

Esteves et al., 2005; Mathys et al., 2005; Nadal-Romero et al., 2009; Wang et al., 2009; Skalak et al., 2010; Lopez-Tarazon et al., 2010). In those areas, erosion processes are mainly driven by the temporal and spatial patterns of precipitations, their nature (i.e., hail, rainfall, snow) and the antecedent soil moisture conditions (Regües and Gallart, 2004; Nadal-Romero et al., 2008). Furthermore, erosion is characterised by strong spatial variations within catchments, associated with the heterogeneity of sediment sources, the presence of a soil cover by vegetation or snow, and the connectivity of sediment sources up to the river network (e.g. Ollesch et al., 2006). Transfer of sediment within rivers is also affected by their specific flow regime (Dedkov and Moszherin, 1992). In mountainous environments, a significant proportion of the total annual discharge can be controlled by the snowmelt occurring in winter and spring (Gallart et al., 2002; Lenzi et al., 2003; Schmidt and Morche, 2006, Mano et al., 2009). An increase in discharge can also lead to an important resuspension of sediment accumulated on the river bed during storms in spring and summer (Navratil et al., 2010). Even though it is widely accepted that different rainfall regimes generate different sediment dynamics patterns and that they involve the contribution of different sediment sources, the relative contribution of those different rainfall regimes to the sediment export from mountainous catchments should be quantified.

This paper aims to analyse the influence of two contrasted rainfall regimes on the mobilisation of sediment sources and the transfer of fine sediment during floods within the 905-km² Bléone catchment located in the Southern French Alps. Widespread rainfall events are characterized by long duration (about a day) but low-intensity rainfall (<20 mm h^{-1}), whereas the heavy storm regime is defined by a short duration (several hours) but a high-intensity (>20 mm h^{-1}). The study catchment is drained by steep-slope torrents and braided rivers (Navratil et al., 2010). This complex type of river is characterised by a wide active channel and the presence of vegetated bars, where the processes of fine sediment deposition,

release and resuspension from the riverbed may be exacerbated. The combination of traditional monitoring techniques (i.e., the installation of river gauges, turbidimeters and sediment samplers in several subcatchments of a larger mountain catchment), rainfall monitoring (i.e., rain gauges, rainfall radar imagery) and sediment tracing (i.e., using radionuclides and elemental geochemistry) could provide valuable information about the temporal variability of substrates supplying sediment and sediment fluxes within this complex mountainous catchment. A recent sediment fingerprinting study conducted in this Alpine catchment quantified the contribution of different sediment sources supplying fine material to the river (Evrard et al., 2011). This study analysed several dozens of composite riverbed sediment samples and showed the important contribution of local sources to sediment deposited on the riverbed. In this paper, we will apply a similar fingerprinting approach on suspended sediment collected during floods, rather than on sediment deposited on the riverbed, to consider intra- and inter-event variation in sediment sources. We will therefore be able to explore temporal variations in sediment source contributions, which was not possible in the previous study. Comparison and integration of results obtained by both studies will finally be discussed to characterise overall spatial and temporal variations of sediment sources in this highly erosive Alpine catchment.

2. **STUDY AREA**

The Bléone catchment (905 km^2), with altitudes ranging between 405 and 2927 m A.S.L. (Above Sea Level), is a mountainous alpine catchment located in the Durance River district, in southeastern France (Figure 1). The catchment is characterised by a dendritic drainage network dominated by the Bléone River and several tributaries, among which the Bès (233

km²-subcatchment), the Arigéol (66 km²), the Duyes (125 km²), the Bouinenc (28 km²) and the Eaux Chaudes (61 km²) Rivers are the most important. A digitised 1:50,000 spatially-distributed geological map of the catchment provided by the French Geological Survey (BRGM) allowed defining the main geological units (Figure 2). The geological bedrock is calcareous (marls, molasses, limestones), with rather large areas of exposed Cretaceous and Jurassic black marls, as well as Lias marly limestones. Severely eroded areas (11% of the Bléone catchment, Figure 2) are defined as zones without vegetation and characterised by the presence of erosion features (e.g., rills, gullies, badland morphology). They were delineated in a GIS using aerial photographs taken during flight campaigns conducted in 2004 by the French National Geographic Institute (IGN). Eroded areas cover a mean surface of 0.45 km² (between 811 m^2 and 1.85 km^2) and were classified into three groups: debris slope areas (22% of the total eroded area), sheet and rill erosion areas (48%) and gully erosion areas (30%). The areas covered by black marls are strongly affected by erosion and they are characterised by a badland morphology, which generally develops in semiarid areas (Mathys et al., 2005; Nadal-Romero et al., 2009). Forest is by far the main land use in the catchment (44% of the total catchment surface; Table 1). Siltation of Malijai reservoir located at the outlet of the Bléone catchment leads to operational problems for hydroelectric power plants located downstream along the Durance River and to an important siltation in the Berre lagoon (Accornero et al., 2008). To limit this problem, French authorities fixed a maximal SSY that can be delivered to the lagoon, which leads to extra management costs for the company exploiting the power plants.

The climate is transitional and undergoes continental and Mediterranean influences. Mean annual temperature ranges between 12–13°C at 400 m A.S.L., with a high temperature range between summer and winter (about 18°C). Mean annual rainfall in the catchment varies between 600–1200 mm at 400 m A.S.L. Rainfall is characterised by important seasonal

variations, with a maximum in spring and autumn (Mano et al., 2009). Two main contrasted rainfall regimes dominate the weather in the Southern French Alps. Widespread rainfall events affect by definition the entire Bléone catchment. They are mainly associated with widespread depressions centred on France, or with Mediterranean fluxes and Western weaker depressions (oceanic influence). Local convective storms and rainfall generated by storm-fronts are generally associated with Eastern fluxes and local air mass instability that affects briefly (i.e., during several hours) very local areas of the catchment (i.e., a few km²). These very short duration and intense events mostly occur between June and September.

Peak flow observed in spring can be accentuated by the snowmelt. In contrast, severe low base flow periods are observed in summer and winter. In winter, the low water stage of the river is mostly explained by the predominance of snowfall (Mano et al., 2009).

3. MATERIALS AND METHODS

3.1. Methodological framework

Rainfall volume (RV) and maximum intensity (RI), river discharges (Q) and Suspended Sediment Concentrations (SSC) were measured at several locations within the Bléone catchment (Figure 1). This monitoring network provided with a high temporal frequency estimations of Suspended Sediment Yields (SSY) and their dynamics during each flood. Suspended sediment samples collected manually or by automatic samplers were analysed by gamma spectrometry (i.e., radionuclides) and by Inductively Coupled Plasma – Mass Spectrometry (ICP-MS; i.e., elemental geochemistry) in order to trace suspended sediment sources during selected widespread rainfall events and local convective storms (Table 2).

Selection was guided by (1) significance and representativeness of the floods according to the hydro-sedimentary regime, and (2) data availability (e.g., suspended sediment sampling during floods without any monitoring problems).

3.2. Rainfall monitoring

Ten rain-gauges managed by the *Laboratoire d'étude des Transferts en Hydrologie et Environnement* (R1–R5) and the French *Cemagref* research agency (R6–R10) provided continuous precipitation records (resolution of ca. 0.2 mm; Figure 1). Five meteorological stations managed by the French meteorological office (i.e., *Météo France*) provided rainfall depths and durations, snow depth, temperature as well as information on the occurrence of storm or hail events (R11–R15). These last stations only provided daily records (with the exception of R12 that provided hourly records).

Rainfall radar images provided by *Météo France* were also available for this region. We used the rainfall estimation provided by the Bollêne (lat.: 04°45'08''E, long.: 44°17'01''N), Nîmes (lat.: 04°21'28''E, long.: 43°50'21''N) and Collobrières (lat.: 06°18'25''E, long.: 43°14'12''N) weather radars (bipolar, doppler, s-band; Figure 1). Low resolution images (with 1 km²-resolution at hourly time-step) were used in this study. These radars are located at more than 60 km from the Bléone catchment, which induced signal mitigation. Moreover, mountain belts probably attenuated the radar waves. Those images were therefore only used to derive qualitative information on the spatial and temporal variability of rainfall, to complement the information provided by the rain gauge network.

3.3. Hydrological and sediment monitoring

River monitoring

Four river gauging stations were installed within the catchment (Table 1, Figure 1). At two stations (Bléone River at Le Chaffaut, i.e. STA1; Bès River at Pérouré, i.e. STA4), flow discharges were provided by the *Electricité de France* (EDF) company and the regional *Flood Forecasting Service* (SPC-Grand Delta; Poirel, 2004; Mano et al., 2009; Navratil et al., 2010). These records are available at a variable time-step, from 1963 at STA4 and from 2000 at STA1. The two other stations (Galabre River at La Robine, i.e. STA 2; Bléone River at Prads, i.e. STA5) were equipped with a 24-GHz radar (Paratronic Crusoe®) to measure the water level with a 10-minutes time-step. Flow discharges were regularly gauged and water level-discharge rating curves were built for each site. At all the four stations, a nephelometric turbidimeter (WTW Visolid® 700-IQ or Hach Lange® at STA1) measured the water turbidity using the backscattering of infrared light.

An additional monitoring station was installed on the Bès River at Esclangon (STA3; Figure 1; Table 1) to monitor SSC only, in order to investigate the transfer of suspended sediment over a short river section located downstream of STA4 (i.e., ca. 5.3 km; Navratil et al., 2010).

At each station, a sequential sampler (ISCO 3700®) containing 24 one-liter bottles was programmed to trigger sampling as soon as critical turbidity thresholds were reached. A data logger (Campbell CR800®) recorded the water level and the turbidity during one minute every 10 minutes. Collected samples were filtered in laboratory using pre-weighed standard Durieux® 0.7-µm-diameter glass microfiber filter paper. The filters were then dried for 2 h at 105 °C and weighed with a high precision balance (uncertainty ± 0.1 mg). In case of high SSC (>2 g l^{-1}), the sample was dried for 24 h at 60 °C and the residue was weighed. A reliable turbidity-SSC calibration curve was built for each station using a polynomial function and it was subsequently used to calculate the SSC time series (e.g. Navratil et al., 2010, 2011; Duvert et al., 2011). Suspended sediment flux SSF [t s^{-1}] was then calculated using Eq. (1).

$$SSF = Q \cdot SSC \quad (1)$$

where Q is the discharge (m^3 s^{-1}) and SSC is the suspended sediment concentration (g L^{-1}). Then, suspended sediment yields (SSY; in tons, t) were calculated for each flood as follows (Eq. 2):

$$SSY = \int_{t_0}^{t_f} SSC \, dt \quad (2)$$

with t_0 and t_f corresponding to the beginning and the end of the period considered.

Uncertainties on SSC monitoring with turbidimeters mainly depend on the turbidity calibration curve, the representativity of the automatic sediment collection by ISCO samplers – i.e., position of the intake in the water flow, SSC homogeneity in the channel cross-section – and the laboratory errors (Lewis and Eads, 2008; Némery et al. 2010). SSY thus cumulate uncertainties on both SSC and discharges. Navratil et al. (2011) showed that global uncertainties reached on average 20% for SSC (range, 1 – 30 %) and 30 % (range, 20 – 50 %) for SSY at STA2 when considering uncertainties of ca. 20% on discharges. In this study, all monitoring stations were installed using the same methodology and in the same physiographic context. We therefore consider that SSC and SSY uncertainties remained in the same order of magnitude at the other stations.

Data analysis

Rainfall events were first characterized by their total volume (mm) and intensity (10 minutes time-step; mm h^{-1}). Rainfall spatial extent and propagation of the rainfall fronts were estimated with radar imagery and information delivered by the raingauge network. Flood timing was defined by analysing flood hydrographs and sedigraphs. In this study, a flood was identified as soon as rainfall occurred in the catchment and triggered sediment transport in the river.

Several flood indicators were estimated: peak discharge (referred to as Qmx); mean annual runoff depth (Qm); baseflow discharge (Qb); mean and maximum suspended sediment concentrations (respectively SSCm and SSCmx); suspended sediment yield (SSY); percentage of total mass of suspended solids and water volume transported during 2% of the monitoring period (Ms2%, V2% respectively; Meybeck et al., 2003); and the fraction of inter-annual sediment yield produced by widespread rainfall events (SSYw).

Floods were also classified according to their Q–SSC hysteretic pattern (i.e., clockwise, anticlockwise or concomitant hysteretic loops), using the categories initially defined by Williams (1989). These patterns provide indeed relevant information to outline the spatial location of sediment sources in the catchment (Williams, 1989; Lenzi and Marchi, 2000; Seeger et al., 2004; Smith and Dragocich, 2008; Duvert et al., 2010). Basically, Q–SSC clockwise patterns are generally attributed to close sediment sources or to the resuspension of fine sediment stored on the river bed or banks. In contrast, Q–SSC anticlockwise patterns would mainly reflect a contribution of sediment sources located at a substantial distance from the outlet. When Q–SSC curves for both hydrograph rising and falling limbs are symmetrical (i.e., concomitant peak), it would reflect that fine sediment availability is never exhausted during the flood; the suspended sediment flux would then only be constrained by the sediment transport capacity of the river. Even though hysteresis analyses provide valuable information to outline the sources of sediment and the timing of its transfer, it is not sufficient to conclude about the sediment origin. We therefore provided additional information derived from sediment fingerprinting, topographical surveys and river monitoring at intermediate stations of the river network to strengthen our findings regarding sediment sources and transfer.

When flood peak propagation could be clearly identified at two successive river monitoring stations, we also estimated the transfer time of SSC peak between both stations. The distance

between the stations was therefore measured using GIS functions to calculate the mean velocity of suspended sediment propagation between successive monitoring stations.

3.4. Analysis of diachronic aerial pictures and topographic survey

Aerial pictures taken at two different dates in 2004 and 2010 by the French National Geographical Institute (IGN) were used to analyse the variations of the lateral margins of the braided channels, and the changing width of the main braided channel. Topographical surveys were also conducted with a total station at three different dates and on three cross-sections (ca. 70 points for each cross-section, located at the main morphological changes). These cross-sections are located along the Bès River (lat.: 44° 11' 14.64"N, long.: 6° 16' 5.72"E) between the Pérouré (STA4) and Esclangon stations (STA3; Figure 1). These data allowed us determining whether significant bed load transport and fine sediment remobilisation occurred during the study period.

3.5. Sediment fingerprinting

Gamma spectrometry analysis

For all the investigated floods, a selection of suspended sediment collected by ISCO samplers was dried and sieved (to 63 µm) before analysis. Selection was conducted in order to analyse sediment transported by floods generated by the representative rainfall regimes occurring in the catchment.

Radionuclides were measured in all the collected samples. Sediment was placed in a counting box containing sufficient material (i.e., 10 g). Radionuclide concentrations (Be-7, Cs-137, excess-Pb-210, K-40, Ra-226, Ra-228, Th-234, Th-228) were determined by gamma-spectrometry using the very low-background coaxial N- and P-types GeHP detectors (Canberra / Ortec / Eurisys) available at the *Laboratoire des Sciences du Climat et de*

l'Environnement (Gif-sur-Yvette, France). Efficiencies and background levels of the detectors were periodically controlled with internal and IAEA soil and sediment standards (Evrard et al., 2011). When there was a very low quantity of material available (i.e., < 10 g), filters were placed in tubes and counting was conducted at the *Laboratoire Souterrain de Modane* in the French Alps, using a very low background, high-efficiency well-type Ge detector (Reyss et al., 1995).

Elemental geochemistry analysis

For the measurement of elemental geochemistry, dried subsamples (ca. 80 mg) were analysed by Inductively Coupled Plasma – Mass Spectrometry (ICP-MS; XII CCT Series, Thermo Electron), in solutions containing 0.2 g of solid L^{-1}. The sediment digestion procedure is described by Le Cloarec et al. (2010). Concentrations were determined for several major (Al, Ca, Mg, Ti) and trace (Ag, Ba, Cd, Cu, Mn, Ni, Pb, Se, Tl, V) elements. Analytical uncertainties associated with this method did not exceed 20% for major elements and 10% for trace elements.

Selection of fingerprints and design of a mixing model

Based on the geological map of the catchment, we grouped the geological classes corresponding to our sediment source samples into six main sediment source types: (1) marly limestones; (2) limy marls; (3) conglomerates and sandstones; (4) Quaternary deposits; (5) black marls and (6) gypsum (see Evrard et al., 2011, for more details on sediment source sampling). Given suspended sediment has a finer grain size than riverbed sediment, in this study we sieved the source material to < 63 µm before characterising their content in radionuclides and geochemical elements (Table 3). We first checked that the properties of the suspended sediment samples remained in the range of the source values. This condition was

not met for Al, Cd and Ti. They were therefore removed from further analysis. The ability of the 19 other potential fingerprinting properties to discriminate between the potential sediment sources was then investigated by conducting a Kruskal-Wallis *H*-test as initially proposed by Collins and Walling (2002). Results outlined 10 potential variables to discriminate the sediment sources (difference significant at $p = 0.05$): Ra-226, Th-234, Ba, Cu, Mn, Ni, Pb, Sb, Tl, V. Based on this set of discriminating properties, an optimum 'composite fingerprint' was identified by performing a stepwise selection procedure. This procedure consisted in minimising Wilk's lambda, as suggested by Collins and Walling (2002). Thus, among those 10 potential variables, 6 properties were sufficient to design the optimum composite fingerprint. Only one geogenic radionuclide was pointed out (Ra-226). The other selected fingerprints were V, Ni, Mn, Sb and Cu. Then, we constructed a Monte Carlo mixing model as already detailed by Evrard et al. (2011) in order to quantify the range of contribution of each sediment source to the suspended sediment samples collected at the different river monitoring stations. The gypsum geological class was removed from the analysis because of its rapid dissolution in the river during floods.

In total, 10,000 random source concentrations were generated by the Monte Carlo mixing model for each suspended sediment sample. The outputs of the mixing model appeared to be very stable, all outputs being very close (and systematically within a range of ± 3%) to their mean value. We therefore decided to only present the mean suspended sediment composition in black marls, limestone/marls, Quaternary deposits and conglomerates.

4. RESULTS

4.1. Inter-annual rainfall, runoff and sediment analysis

341 Among the 196 rainfall events that occurred in the Bléone catchment between October
342 2007 and December 2009, about one-third of them generated suspended sediment that was
343 recorded by our river monitoring stations. The monitored hydrological years Oct. 2007– Sept.
344 2008 and Oct. 2008 – Sept. 2009 were rather wet (870 mm and 930 mm, respectively) when
345 compared to the mean annual rainfall depth recorded from 1934 to 2009 (i.e., 820 mm yr^{-1};
346 data from raingauge R15; Figure 1). Rainfall increased with altitude (i.e., orographic effect)
347 and was strongly heterogeneous within the catchment, depending on the dominant weather
348 regime. Mean annual runoff depth remained relatively constant during the two monitored
349 years because of the relatively equivalent rainfall inputs.
350
351 On average, widespread rainfall events are longer (20 hours at R2) than storm events (6 hours
352 at R2). Both rainfall regimes are rather well discriminated (Figure 4): storms are generally
353 associated with higher intensities (>20 mm h^{-1}). Widespread events are associated with a high
354 rainfall volume (up to 120 mm), but with low-moderate intensities (<20 mm h^{-1}). Storms can
355 be particularly heavy and they can affect very local areas, with much higher rainfall
356 intensities (maximum of 162 mm h^{-1} with 10-minutes time-step rainfall data at R1). These
357 events are sometimes accompanied with hail.
358
359 All the results outline a strong seasonality and inter-annual variability of SSY in the Bléone
360 catchment (Figure 3a and 6). Our monitoring at the different stations showed that 75 – 99.9%
361 of the total sediment yield were produced during ca. 2% of time and transported at each
362 station by less than 18% of the total water volume (Ms2% and V2%; Table 4). Furthermore,
363 30–70% of total SSY (respectively at STA2 and STA4) were transported during the last three
364 months of the study (Oct. 2009 – Dec. 2009; Figure 3a). These results show the strongly
365 episodic behaviour of suspended sediment transport in the Bléone catchment.

SSY measured on the Bléone River at STA1 (close to the catchment outlet) between Oct. 2007 and Dec. 2009 reached 641,900 ± 192,600 tons (Table 4). This value corresponds to an inter-annual specific sediment yield (SSY*) of 330 ± 100 t km^{-2} yr^{-1}. However, SSY* were found to fluctuate within the Bléone catchment; they varied indeed between 452 ± 136 t km^{-2} yr^{-1} on the Bléone at Prads (STA5) and 690 ± 200 t km^{-2} yr^{-1} on the Bès River (STA4). Higher SSY* (more than 5,000 t km^{-2} yr^{-1}) were observed at Draix in smaller subcatchments (Mathys et al., 2003). Those rates remained in the same order of magnitude as the ones observed in other similar mountainous catchments (e.g. López-Tarazón et al., 2009). The difference in sediment yields observed between Oct. 2007 – Sept. 2008 and Oct. 2008 – Sept. 2009 (100–700% variation; Figure 3a) can partly be explained by the presence of a deep and persistent snow cover during the 2009 winter and spring seasons, which probably protected the soil against erosion.

Sediment yields recorded in all the monitored subcatchments were mainly generated by widespread rainfall events (SSYw ranges, 72–89 %). The upper Bléone (STA5) subcatchment was more affected by storms than the other stations probably because of its higher altitude.

Interannual analysis masks strong annual variations: in Oct. 2007 – Sept. 2008, the bulk of the sediment yield was mainly attributed to S–W Mediterranean depressions that generated widespread rainfall, whereas between Oct. 2008 and Sept. 2009, convective storms (local storm or storm-front) dominated and produced 70% of sediment. For instance, between Oct. 2007 and Sept. 2008, convective storms produced 70% of the annual SSY at STA4. In contrast, during the Oct. 2008 – Sept. 2009 period, widespread Mediterranean events produced 67% of the sediment transport recorded at the same station. The rest (i.e., 23%) was generated by storms that mainly occurred in the upstream parts of the catchment monitored at

391 Pérouré (STA4) and Prads stations (STA5). Seven hail storms were reported at the Seyne
392 station (1300 m A.S.L.) between Oct. 2008 – Sept. 2009, but only four between Oct. 2007 –
393 Sept. 2008, which indicates the more frequent occurrence of heavy storms in spring and
394 summer 2009.
395
396 Convective storms generate lower peak discharges (Qmx) than widespread events at STA1
397 and STA4 (Wilcoxon rank sum test; p-value<0.05). At STA2 and STA5 stations (i.e.
398 headwater catchment), mean Qmx was higher during widespread events than during storms,
399 even though this difference is not significant (p-value>0.4). This difference could be
400 explained by the local pattern of rainstorms. Differences between distributions of maximum
401 suspended sediment concentrations (SSCmx) during widespread events and local storms were
402 not significant for all the monitoring stations (Wilcoxon rank sum test; p-value>0.9). The
403 difference between both rainfall regimes was only significant for the flow discharge indicator
404 at a larger catchment scale (713 km² at STA1 and 165 km² at STA4). We can hypothesize
405 that, at larger spatial scales, important sedimentation can occur in braided rivers during
406 storms, given that the flow is not able to transfer as much sediment as during widespread
407 floods. Field observations showed that storms generate significant sedimentation along the
408 river network, and particularly in braided channel reaches (Navratil et al., 2010). Those
409 deposits probably provide the bulk of the total SSY during widespread rainfall events that
410 generate higher flow discharges in the rivers.
411
412 Q–SSC hysteretic patterns tend to confirm the importance of those sedimentation/erosion
413 processes along the river network (Figure 3b). On the Upper Bléone River at STA5 station,
414 anticlockwise hysteretic loops were the main patterns controlling the sediment export. This
415 would mean that the bulk of suspended sediment was rapidly transported from highly erodible

areas to the outlet (during a single flood), and that only limited sediment amounts were stored in the river channel. In contrast, at STA2 station, sediment storage on the riverbed and remobilisation would be more important, given that 40% of sediment was delivered by clockwise events at this location. However, this pattern could also be attributed to the delivery of sediment sources located in the vicinity of the gauging station. At STA1 and STA4 stations, floods with clockwise hysteresis patterns were the most frequent (Figure 3c) and they transported the bulk of the annual sediment load (>80% of annual SSY). Sediment dynamics were then probably mainly controlled by the remobilisation of fine sediment from the large and well-developed braided river channels that can be observed in this river section.

Overall, the relative contribution of direct sediment supply to the river and sediment remobilisation from the channel to the total sediment exports from the catchment would mainly be explained by the type of rainfall regime that strongly influences the hydraulic conditions and thus the suspended sediment dynamics. The variability of erosion and sediment transfer processes probably explains part of the observed variability affecting the SSY–Qmx relationship at the different stations (Figure 5). In the next sections, we propose to focus our detailed analyses on a selection of widespread rainfall events recorded in the entire catchment (section 4.2) and on a selection of storms (section 4.3; Table 2; see the timing of the studied flood on Figure 6).

4.2. Detailed analysis of widespread rainfall events

We chose two representative events (Figures 4, 7) to illustrate the variety of sediment erosion/transport processes observed in this mountainous catchment (Figures 6; Table 4): (1) a major flood that occurred on 22 December 2009 on the Bès River and monitored at STA4

(referred to as case W1); (2) a comparison of three floods that occurred between 31 October 2008 and 12 November 2009 on the Galabre River and recorded at STA2 (case W2a/b/c).

Case W1: Analysis of the 22 December 2009 flood on the Bès River at Pérouré (STA4)

This 10-yr return period flood was recorded at STA4 (Qmx = 140 $m^3 s^{-1}$; Table 4; Figure 7). It was the second largest flood observed in the Bléone catchment during the 27-months monitoring period (Figures 5, 6). The return period of this flood is probably lower downstream than in upstream subcatchments (i.e., Bès) because of a strongly heterogeneous rainfall pattern. The flood occurred after a succession of 6 low-intensity floods in autumn. It was followed two days later by a 15-yr return period flood (Qmx = 180 $m^3 s^{-1}$). These floods were generated by a rapid air temperature warming associated with a wet Mediterranean South-Western depression, when the catchment was covered by a substantial snow layer. Minimum daily temperature increased indeed from –12°C to +5°C within four days (data from the R15 station). Rainfall volume was very important (108 mm during one day; Figure 7c), but rainfall intensity remained low (20 mm hr^{-1}). Rainfall was distributed homogeneously over the Bès subcatchment, upstream of STA4 (Figure 7a). Sediment export at the outlet reached 57,500 ± 17,500 tons, i.e., 50% of the mean annual SSY. Its contribution to the total SSY produced during the 27-months monitoring period was significant at all the stations (Figure 6). Transfer time of the SSC peaks between the Bès River at Pérouré (STA4) and the Bléone River at Le Chaffaut (STA1) stations reached about 4 hours, with a mean flow velocity of about 1.8 m s^{-1}. Mean flow velocity estimated from STA4 to STA5 was higher (3 m s^{-1}), showing a significant slow-down of the sediment propagation that could be associated with the river bed slope decrease (from 1.4% at STA5 to 0.8% at STA1).

Q–SSC relationship during this flood is characterised by a well-marked clockwise hysteretic pattern (Figure 7e) that reflects a rapid contribution of sediment sources to the outlet. After

465 the flood rising phase, SSC remained stable (at ca. 25 g l^{-1}) and did not vary with discharge
466 anymore, which probably indicates a significant remobilisation of riverbed sediment.
467 Six suspended sediment samples were analysed to outline the potential variations of sediment
468 origin during the flood (Table 5; Figure 7d). We observed a major contribution of black marls
469 (45%) during the rising phase of the hydrograph that can be attributed to a contribution of
470 black marl sources located close to the outlet and that were first eroded during the rainfall
471 front propagation from the southwest to the northeast. During the flood peak that coincided
472 with the maximum sediment transport, sediment was provided by the different lithological
473 sources available along the river network, i.e. black marls (mean, 33%), limestones/marls
474 (mean, 25%), Quaternary deposits (mean, 24%) and conglomerates (mean, 18%); Figure 7d).
475 Overall, contribution of the different sources corresponded to their occurrence in the draining
476 catchment (Figure 2).
477 Sediment composition was stable during the flood (Figure 7d). When considering the
478 contribution of those lithological variations to the sediment yield, we observe that the mean
479 sediment composition at the flood scale is very similar to the sediment composition of the
480 flood peak sample (< 4% of difference). Sediment composition of the flood peak could
481 therefore be usefully used as an indicator of sediment composition during widespread events.
482 Q–SSC clockwise hysteresis (Figure 7e) corroborates the results obtained from aerial picture
483 analysis and topographical surveys conducted before and after this flood on the Bès River
484 between STA4 and STA5 (Figure 8a) along three cross-sections (T1–T3). River bed erosion
485 was found to reach a mean of 34 cm at T3 and 4 cm at T1 location, and erosion depth reached
486 up to 1.5 m at other locations. Furthermore, a diachronic comparison of aerial pictures (Figure
487 8c) shows that the main channel has significantly divagated within the entire braided channel,
488 which completely modified all braided river morphological features (i.e., gravel bars, braided
489 channels, vegetated bars and river banks; Figure 8a). Bank erosion was found to fluctuate

between about 5 m at T1 (Figure 8b) and up to 50 m at several locations in the reach (Figure 8c). These values corroborate the ones obtained by previous topographical measurements and the outputs of a LiDAR analysis conducted on a 7-km long reach of the Bès River (Tacon et al., 2011). Navratil et al. (2010) estimated that fine sediment concentration deposited in a braided river reach (between STA4 and STA5) represented a mean of 7 kg m^{-2} per 10 cm depth. If we hypothesise that the braided channels located upstream of station SAT5 (about 730,000 m^2 on the Bès and its tributaries) was disturbed over a mean of ca. 0.6–1.5 m depth, we can estimate that 80–100% of SSY (i.e. 57,500 ± 17,500 tons) were remobilised from the riverbed and the river banks.

Case W2: Inter-flood analysis on the Galabre River at La Robine (STA2) between 31 October 2008 and 12 November 2008

Those three autumnal floods were generated by a central and southwestern depression that generated a moderate rainfall volume with a low intensity (about 15 mm hr^{-1}; Table 4; Figure 9). Snowfall occurred above 1500 m ASL (data from R15 meteorological station). Precipitation was distributed homogeneously across the Galabre subcatchment (Figure 9a, c). Those events occurred after a succession of storms in summer and early in autumn that generated very high SSC (up to 130 g l^{-1}), but low-moderate peak discharges (<2.2 m^3s^{-1}). River capacity was then probably insufficient to transport all the suspended sediment down to the outlet. A significant proportion of this sediment probably deposited along the trunk river and the tributaries. Those deposits hence constituted an important source of fine sediment that was made easily available during the 2008 autumn floods. SSY exported by those 3 events correspond to ca. 6 % of the mean annual sediment yield in this subcatchment (Figure 9a).

Sediment was mainly provided by limestones/marls (20-31%) and black marls (50-61%). Overall, those contributions remained stable throughout the period, even though the

515 dominance of black marls was particularly observed during the 12 November flood which
516 was characterised by a sharp rising limb (Figure 9). As shown in case study W1, we
517 hypothesise that the composition of those flood peaks is representative of the mean sediment
518 composition during the flood in terms of SSY.
519 We observed a concomitant Q–SSC pattern during the first flood, a clockwise pattern during
520 the second flood and two concomitant patterns during the third flood (Figure 9d). It probably
521 reflects a significant remobilisation of fine sediment stored on the riverbed during summer.
522 During the second flood, we observed a stabilisation of SSC at ca. 30 g L^{-1} during the flood
523 rising limb. As for case W1, this phenomenon can be attributed to a high and rapid
524 remobilisation of fine sediment from the riverbed. Sediment availability was probably never
525 exhausted during these periods. Each of these three floods was characterised by several (2–4)
526 SSC peaks (Figure 9a). Magnitude of these intra-event peaks systematically decreased,
527 whereas peak discharges remained stable or even increased. These observations outline a
528 rapid supply or "first-flush" of fine sediment that was probably stored in the river network
529 and easily available (Lawler et al., 2006), followed by the sediment supply by remote sources,
530 and finally by the occurrence of sedimentation in the main channel during the falling limb of
531 the flood.
532
533 **4.4 Analysis of local storms**
534 Storms generally affected local areas and mainly occurred in upstream parts of this
535 mountainous catchment. For instance, 28 local convective storms were recorded in 2009 by
536 the Seyne raingauge (R15; 1550 m ASL) vs. only 3 events by the Digne raingauge (R12; 550
537 m ASL). These events mainly affected small but highly erodible upstream areas. They even
538 generated debris flows in some torrents.

We analysed three floods characterised by different spatial patterns (Table 2; Figure 6): (1) a storm that occurred in the Galabre subcatchment (case S1); (2) the propagation of a flood wave from the summits of the Upper Bléone subcatchment at STA5 down to the Bléone catchment outlet (case S2); (3) and the contribution of a small tributary, the Aigue-Belle torrent (draining about 4 km²) to the total sediment yield generated by a storm on the Bès River between 2 successive monitoring stations (i.e., STA3 and STA4) separated by ca. 5 km (case S3).

Case S1: 12 August 2008 storm on the Galabre River at La Robine (STA2)

A convective summer storm occurred in the Galabre subcatchment on 12 August 2008 (Figure 10a; Table 4). It corresponds to the most important storm recorded during the 27-months monitoring period at this station, with a total rainfall depth of 24 mm and an intensity of 90 mm hr^{-1} (partly accompanied with hail). Significant sediment loads were recorded (638 ± 190 tons) at STA2, representing ca. 4% of the mean annual SSY at this location. Similar storms occurred at many other locations of the Bléone catchment and generated significant but variable SSY characterised by different temporal patterns. Total SSY recorded in the Bléone upstream subcatchments reached 3,200 ± 1000 tons whereas the total export at STA1, close to the outlet, was estimated at 1,300 ± 400 tons (Figure 6). This difference outlines a significant storage of fine sediment within the braided river network (i.e., at least 1,900 ± 600 tons during this storm).

Black marls supplied a large but progressively decreasing part of sediment during the flood rising stage (from 48% to 34%; Figure 10d). Then, sediment contribution from Quaternary deposits clearly dominated (52% to 78%; Figure 10d). Q–SSC relationships were characterised by the succession of a clear anti-clockwise pattern (Figure 10c; A2–A5). The first SSC peak can mainly be attributed to the direct supply of sediment generated by close

564 black marl sources (Figure 2). In contrast, the second peak was supplied by remote
565 Quaternary deposit sources in the catchment.
566
567 **Case S2: The 30 June 2009 flood that propagated along the entire Bléone catchment**
568 The 30 June 2009 storm corresponds to a heavy eastern storm-front associated with hail falls
569 (Figure 11a). It was mainly observed at STA5 (Figure 11a, b, c), but it also affected the Bès
570 and Galabre River subcatchments even though it was less important in those latter areas. This
571 storm produced 1,000 ± 300 tons of sediment recorded at STA5 (i.e. more than 3% of the
572 mean annual SSY); 1,500 ± 450 tons at Pérouré (i.e., 1%); 44 tons at La Robine (i.e., 0.5%)
573 and 600 ± 180 tons at STA1. At least 1,900 ± 600 tons of sediment were therefore stored in
574 the river channel during this flood. SSC peak propagated from STA5 to STA1 (Figure 1) in
575 about 6.5 hours with a mean velocity of about 1.7 m s^{-1}.
576 This flood mainly mobilized the upstream sediment from Prads down to the outlet (see for
577 instance the source contribution similarity of C3 sample – collected at upstream Prads station
578 – and C5 sample – collected at the catchment outlet; Figure 11d) during the flood peak.
579 Sediment composition (i.e., dominance of black marls and marly limestones) determined at
580 Robine (STA2) and Pérouré (STA4) stations was different, but their contribution to the total
581 sediment export was minor (Figure 11d). The source contribution at the outlet (STA1; C6)
582 during flood recession is found to be very consistent with these subcatchment contributions
583 (C2, C4) and confirms their late contribution to the suspended sediment yield. Anticlockwise
584 or concomitant patterns at each station confirm that the bulk of sediment was provided by
585 hillslope erosion and by a direct propagation of sediment down to the catchment outlet.
586
587 **Case S3: The 7 August 2009 flood on the Bès River at Pérouré (STA4) and Esclangon**
588 **stations (STA3)**

589 A convective summer storm occurred in the Bès and Upper Bléone subcatchments on 7
590 August 2009 (Figure 12a). It generated a total rainfall depth of 55 mm with an intensity of 57
591 mm hr^{-1} (without hail). This event was even more local than the two events detailed
592 previously, and it did not affect the other subcatchments (Figure 5). About 3,900 ± 1,200 tons
593 were exported by the Bès River at STA4 (ca. 3.5% of mean annual SSY) and 170 ± 50 tons
594 (i.e., 0.5%) were exported by the Bléone River at STA5. 1,700 ± 500 tons of sediment
595 reached the outlet at SAT1 (i.e. less than 1% of annual SSY). We can therefore estimate that
596 at least 2,400 ± 700 tons of sediment deposited on the riverbed. Suspended sediment
597 propagated from Pérouré (STA4) to Esclangon (STA3) with a mean velocity of about 0.7 m s^{-1}
598 ; which is very low compared to the mean propagation of 3 m s^{-1} observed during the 22
599 December 2009 flood (case W1).
600 We also analysed suspended sediment collected during this event at two stations (STA4 and
601 STA3). Three samples corresponding to different positions in the hydrograph (i.e. rising limb,
602 peak, falling limb) were analysed at each station. It is generally assumed that the bulk of
603 sediment transported during an anticlockwise flood originates from distant sources. This is
604 confirmed by the results obtained for the anticlockwise flood sampled at both STA3 and
605 STA4 (Figure 12). Black marls provided indeed 60–70% of sediment during peak flow.
606 According to the geological map of the Bléone catchment (D2 and 3 samples; Figure 2), there
607 is an important presence of black marls in the upstream part of the Bès subcatchment. The
608 composition of the sediment at the downstream station is very similar (D5, D6), indicating the
609 transfer of this sediment and the conservation of the sediment composition. In contrast, at the
610 beginning of the flood, the important contribution of conglomerates and Quaternary deposits
611 supplied by a small but very active torrent significantly modified sediment composition
612 between STA4 and STA3 (i.e., Aigue-Belle torrent; Figure 12d).
613

5. GENERAL DISCUSSION

5.1. Influence of rainfall regime on temporal variability of sediment origin

Overall, widespread flood events transported the bulk of SSY (72–89%) in the Bléone catchment during the 2007-2009 period. Convective storms generated lower discharges than widespread events in the downstream monitored rivers. They were generally associated with high suspended sediment concentrations and were associated with a high sedimentation in the river channel. At the downstream stations, floods with clockwise Q–SSC hysteresis transported the bulk of sediment, indicating an efficient re-suspension of the fine sediment stored on the riverbed.

Black marl/limestone contribution was found to be very large during both storms and widespread rainfall events. Given that those later events produce a much higher proportion of the total sediment fluxes exported from the entire catchment, black marls contribute to 30−61% of the global sediment export. Quaternary deposits (molasses) and limestone/marl contributions were also significant. These sources covered the bulk of the catchment surface (89%) and supplied also a significant fraction of sediment.

5.2. Relative contribution of channel sediment and wash load

Wash load is generally defined as the fraction of sediment transported in suspension from sources up to the outlet having no or little interaction with the river bed or banks. Our results put into question the relevance of this concept in mountain catchments. Topographic surveys and Q-SSC hysteresis analysis provided consistent results and showed that there was a significant contribution of fine sediment remobilised from the river channel to the global sediment export during widespread events. Fine sediment recharge in the river network would

mainly occurs (1) during storms characterised by low discharges but very high SSC or (2) during the falling limb of the flood hydrograph, with sand-sized particle sedimentation in braided channels and silt/clay-sized infiltration in the gravel bed layer. Further studies should focus on inter-flood weather patterns – freezing–heating cycles, hail occurrence, soil moisture – and their effect on sediment erosion (e.g. Yamakoshi et al., 2009), as well as on the sediment size and on sediment degradation processes that occur during sediment transfer between hillslopes and the catchment outlet.

5.3. Composition of suspended sediment vs. riverbed sediment (as determined by Evrard et al., 2011)

Figure 13 provides a general comparison of substrate composition in the area draining to each river monitoring station of the Bléone catchment, and to the corresponding composition derived from sediment fingerprinting conducted on both riverbed material (Evrard et al., 2011) and suspended material (this study) collected at each station. Overall, our results showed a systematic over-representation of black marls (i.e., more erodible sources) and an under-representation of limestones (i.e., less erodible material) in sediment. An over/under-representation refers here to the contribution that might be expected based on the relative proportion of the catchment occupied by a particular rock type. In contrast, sediment supply by Quaternary deposits and conglomerates better corresponds to the surface that they occupy in the different draining catchments. At Pérouré station on the Bès River (STA 4; Figure 13a), the bulk of riverbed sediment is supplied by conglomerates and Quaternary deposits (Evrard et al, 2011). This result is logical in the sense that limestones are less erodible. In suspended sediment, we observed in contrast a mix of the different sources, with an over-representation of limestones and black marls. Those source materials are probably exported by the finest

sediment fraction. In the Galabre subcatchment (at Robine station; STA2; Figure 13b), the bulk of riverbed sediment is supplied by black marls (77%; Evrard et al, 2011), the remaining part being supplied by limestones. In suspended sediment, this trend is confirmed, with an important additional contribution of Quaternary deposits. These results are consistent with a recent study conducted on the same flood with the DRIFTS approach (Poulenard et al., in review). Both methods show a large contribution of black marls during the first rising limb (providing 47% of sediment according to this study vs. 67% after Poulenard et al., in review) and an important contribution of limestones (30% vs. 18%) and Quaternary deposits (15% vs. 15%). During the second part of the flood characterised by a sediment supply by remote sources, the contribution of black marls (24% vs. 59%) and limestones (12% vs. 5%) decreased, whereas the contribution of Quaternary deposits increased (60% vs 35%). We need to outline that we have considered the same flood, but not the same sediment samples (event S1; 12/08/2009), which can partly explain the contribution differences existing between both approaches.

At Prads, in the Upper Bléone River (Figure 13c), we outlined the dominant contribution of Quaternary deposits and conglomerates in riverbed sediment (Evrard et al., 2011) vs. the dominance of limestones and Quaternary deposits in suspended sediment. This contribution difference would reflect the fact that riverbed sediment is composed of coarser material (with a larger proportion of sand-sized material derived from conglomerates and sandstones) than suspended sediment (with a larger proportion of finer material derived from marls).

At the Bléone outlet (Malijai station; Figure 13d) the contribution of the four lithologies observed in the entire catchment to riverbed sediment and to suspended sediment is much more comparable to the surface of the different lithologies observed in the catchment than at the upstream stations. Those results show the particularly large sediment supply by black marls. They also confirm that conglomerates are mostly exported in the form of riverbed

689 sediment, whereas the bulk of black marls/marly limestones are exported in the form of
690 suspended sediment.

691

692 **5.3. Implications for river management**

693 Suspended sediment fingerprinting outlined the very important contribution of black
694 marls during both widespread and storm events, although they only cover ca. 10% of the total
695 catchment surface. Contribution of limestones/marls to the catchment sediment export during
696 widespread events is also important (case W1, W2).
697 This finding corroborates the results obtained by the spatial analysis conducted by Evrard et
698 al. (2011) and has important management implications. Because of locally very high erosion
699 rates in terrains covered by black marls, erosion mitigation was concentrated in those areas
700 (e.g., Rey, 2009). Our results confirm that these restoration works are crucial to control
701 erosion in this catchment where black marls dominate. However, at the entire catchment
702 scale, this study also outlined the significant supply of sediment by limestone/marly terrains
703 to the river as well as the significant contribution of Quaternary deposits and conglomerates
704 (21-79% for the investigated widespread floods).

705

706

707 **6. CONCLUSION**

708

709 This study, conducted in a 905-km^2 mountainous catchment of the southern French Alps,
710 combined the use of a river monitoring network – gauging stations, raingauges, radar imagery
711 – and sediment fingerprinting using radionuclide and elemental geochemistry concentrations
712 as input properties to a Monte Carlo mixing model. Our results showed the strong diversity of
713 the erosion processes involved in the catchment at the different spatial scales considered (22 –

713 km²). It also outlined the dominant control of the rainfall regimes on the erosion and sediment transfer processes. During the study period (Oct. 2007 – Dec. 2009), erosion rates reached a mean of 330 ± 100 t km^{-2} yr^{-1} in the Bléone catchment, but they strongly fluctuated between the different subcatchments (85 – 5000 t yr^{-1} km^{-2}). Sediment exports generated by local convective storms varied significantly at both intra- and inter-flood scales because of spatial heterogeneity of rainfall. However, black marl/marly limestone contribution remained systematically high. In contrast, widespread lower intensity rainfall events that generate the bulk of annual sediment supply at the outlet were characterised by a much stable lithologic composition and by a larger contribution of limestones/marls, Quaternary deposits and conglomerates, which corroborates the results of a previous sediment fingerprinting study conducted on riverbed sediment collected in this catchment. This study also outlined the importance of fine sediment storage in the river network and the major contribution of the re-suspension of those deposits and/or the supply of channel bank material to the bulk of sediment exported during widespread events. This finding raises questions about the relevance of the washload concept in mountain rivers. Further research should focus on the use of fallout radionuclides (e.g., Be-7, excess-Pb-210; Evrard et al., 2010) with a higher spatial and temporal frequency to better understand sediment dynamics within the river network. *In situ* suspended sediment-size monitoring could also be performed to further investigate the mechanisms of sedimentation and degradation of the different sediment types within the catchment. Our results strongly defend the use of a combination of different techniques to get more insight on the origin and the dynamics of sediment in highly erosive mountainous catchments.

Acknowledgements

This work was conducted in the framework of the STREAMS (*Sediment TRansport and Erosion Across Mountains*) project funded by the French National Research Agency (ANR/ BLAN06-1_139157). The authors would like to thank Juliette Montaigu for her help to prepare and analyse suspended sediment by ICP-MS, as well as Fred Malinur, Lucas Muller and Amélie Douchin for the installation of the monitoring stations and/or for their assistance during the field campaigns. Finally, the authors are grateful to two anonymous reviewers for their comments that greatly improved the quality of this manuscript.

REFERENCES

Accornero, A., Gnerre, R., Manfra, L., 2008. Sediment concentrations of trace metals in the Berre lagoon (France): an assessment of contamination. *Archives of Environmental Contamination and Toxicology*, **54**: 372–385.

Carpenter, SR., Caraco, NF., Correll, DL., Howarth, RW., Sharpley, AN., Smith, VH., 1998. Nonpoint pollution of surface waters with phosphorus and nitrogen. *Ecological Application* **8**(3): 559–568.

Collins, A., Walling, D., 2002. Selecting fingerprint properties for discriminating potential suspended sediment sources in river basins. *Journal of Hydrology*, **261**: 218-244.

Collins, A.L., Walling, D.E., Leeks, G.J.L., 2005. Storage of fine-grained sediment and associated contaminants within the channels of lowland permeable catchments in the UK. In *Sediment Budgets 1*, Walling DE, Horowitz A (eds). IAHS Publication No. 291. IAHS Press, Wallingford: 259–268.

Dedkov, AP., Moszherin, V.I., 1992. Erosion and sediment yield in mountain regions of the world. Erosion, debris flow and environment in mountain regions. *IAHS publication* 209, 29-36.

763 Droppo, IG., 2001. Rethinking what constitutes suspended sediment. *Hydrological Processes*
764 **15**: 1551–1564.
765 Duvert, C., Gratiot, N., Evrard, O., Navratil, O., Prat., C., Esteves, M., 2010. Drivers of
766 erosion and suspended sediment transport in three headwater catchments of the Mexican
767 Central Highlands. *Geomorphology*, **123**: 243-256.
768 Duvert, C., Gratiot, N. Nemery, J., Burgos, A., Navratil, O. 2011. Sub-daily variability of
769 suspended sediment fluxes in small mountainous catchments – Implications for community
770 based river monitoring. *Hydrology and Earth System Sciences.* 15 (3) 703–713. doi:
771 10.5194/hess-15-703-2011.
772 Esteves, M., Descroix, L., Mathys, N., Lapetite, J., 2005. Field measurement of soil hydraulic
773 properties in a marly gully catchment (Draix, France). *Catena*, **63** (2-3): 282-298.
774 Evrard, O., Navratil, O., Ayrault, S., Ahmadi, M., Némery, J., Legout, C., Lefèvre, I., Poirel,
775 A., Bonté, P., Esteves, E., 2011. Combining suspended sediment monitoring and
776 fingerprinting to trace the spatial origin of fine sediment in a mountainous river catchment,
777 *Earth Surface Processes and Landforms* 36, 1072-1089.
778 Evrard, O., Némery, J., Gratiot, N., Duvert, C., Ayrault, S., Lefèvre, I., Poulenard, J., Prat, C.,
779 Bonté, P., Esteves, M., 2010. Sediment dynamics during the rainy season in tropical
780 highland catchments of central Mexico using fallout radionuclides. *Geomorphology*, **124**:
781 42-54.
782 Gallart, F., Llorens, P., Latron, J., Regües, D., 2002. Hydrological processes and their
783 seasonal controls in a small Mediterranean mountain catchment in the Pyrenees. *Hydrology*
784 *& Earth System Science* **6**, 527-537.
785 Gottardi., F., 2009. Estimation statistique et réanalyse des précipitations en montagne.
786 Utilisation d'ébauches par types de temps et assimilation de données d'enneigement.

787 Application aux grands massifs montagneux français. *unpublished PhD thesis* ; INP
788 Grenoble. 284p.
789 House, WA., Warwick, MS., 1999. Interactions of phosphorus with sediments in the River
790 Swale, Yorkshire, UK. *Hydrological Processes*, **13**: 1103–1115.
791 Lawler, D.M., Petts, G.E., Foster, I.D.L., Harper, S., 2006. Turbidity dynamics during spring
792 storm events in an urban headwater river system: The Upper Tame, West Midlands, UK
793 *Science of the Total Environment*, **360**: 109– 126
794 Le Cloarec, M.F., Bonté, P., Lefèvre, I., Mouchel, J. M., Colbert, S., 2007. Distribution of
795 ^{7}Be, ^{210}Pb and ^{137}Cs in watersheds of different scales in the Seine River basin: Inventories
796 and residence times. *Science of the Total Environment*, **375** (1-3), 125-139.
797 Le Cloarec, M.F., Bonté, P.H., Lestel, L., Lefèvre, I., Ayrault, S., 2010. Sedimentary record
798 of metal contamination in the Seine River during the last century. *Physics and Chemistry of*
799 *the Earth, Parts A/B/C.* doi:10.1016/j.pce.2009.02.003
800 Lenzi, M.A., Marchi, L., 2000. Suspended sediment load during floods in a small stream of
801 the Dolomites (Northeastern Italy). *Catena* **39**: 267-282
802 Lenzi, M. A., Mao, L., Comiti, F., 2003. Interannual variation of suspended sediment load
803 and sediment yield in an Alpine catchment. *Hydrological Sciences Journal*, **48**, 899-915.
804 Lewis, J. and Eads, R., 2008. Implementation guide for turbidity threshold sampling:
805 principles, procedures, and analysis. Gen. Tech. Rep. PSW-GTR-212. Albany, CA: U.S.
806 Department of Agriculture, Forest Service, Pacific Southwest Research Station, 86 p.
807 López-Tarazón, J.A., Batalla, R.J., Vericat, D., Francke, T., 2009. Suspended sediment
808 transport in a highly erodible catchment: The River Isábena (Southern Pyrenees).
809 *Geomorphology*, **109**: 210–221.

Lopez-Tarazon, J. A., Batalla, R. J., Vericat, D., Balasch, J. C.. 2010. Rainfall, runoff and sediment transport relations in a mesoscale mountainous catchment: The River Isábena (Ebro basin). *Catena* 82: 23–34

Mano, V., Nemery, J., Belleudy, P., Poirel, A., 2009. Assessment of suspended sediment transport in four Alpine watersheds (France): influence of the climatic regime. *Hydrological Processes* **23**, 777-792.

Mathys, N., Brochot, S., Meunier, M., Richard, D., 2003. Erosion quantification in the small marly experimental catchments of Draix (Alpes de Haute Provence, France). Calibration of the ETC rainfall–runoff–erosion model. *Catena*, **50**: 527– 548

Mathys, N., Klotz, S., Esteves, M., Descroix, L., Lapetite, J., 2005. Runoff and erosion in the Black Marls of the French Alps: Observations and measurements at the plot scale. *Catena*, **63** (2-3): 261-281.

Mathys, N., 2006. Analyse et modélisation à différentes échelles des mécanismes d'érosion et de transport de matériaux solides : Cas des petits bassins versants de montagne sur marne (Draix, Alpes-de-Haute-Provence). unpublished PhD thesis ; INP Grenoble. 346p.

Meybeck, M., Laroche, L., Dürr, HH., Syvitski, JP., 2003. Global variability of daily total suspended solids and their fluxes. *Global Planetary Changes*, **39**: 65–93.

Nadal-Romero, E., Regues, D., 2009. Detachment and infiltration variations as consequence of regolith development in a Pyrenean badland system. *Earth Surface Processes and Landforms*. 34 (6), 824-838. DOI 10.1002/Esp.1772

Navratil, O., Legout, C., Gateuille, D., Esteves, M., Liebault, F., 2010. Assessment of intermediate fine sediment storage in a braided river reach (Southern French Prealps), *Hydrological Processes*, DOI: 10.1002/hyp.7594.

Navratil, O., Esteves, M., Legout, C., Gratiot, N., Nemery, J., Willmore, S., Grangeon, T., 2011. Global uncertainty analysis of suspended sediment monitoring using turbidimeter in a

small mountainous river catchment, *Journal of Hydrology*. **398**: 246–259 DOI:10.1016/j.jhydrol.2010.12.025.

Némery, J., Mano, V., Navratil, O., Gratiot, N., Duvert, C., Legout, C., Belleudy, P., Poirel, A., Esteves, M., 2010. Feedback on the use of turbidity in mountainous rivers. Retour d'expérience sur l'utilisation de la turbidité en rivière de montagne. *Tech. Sci. Méthodes*. **1/2**:61-67

Ollesch, G., Kistner, I., Meissner, R., Lindenschmidt, K. E., 2006. Modelling of snowmelt erosion and sediment yield in a small low-mountain catchment in Germany. *Catena,* **68** (2-3), 161-176.

Owens, P.N., Batalla, R.J., Collins, A.J., Gomez, B., Hicks, D.M., Horowitz, A.J., Kondolf, G.M., Marden, M., Page, M.J., Peacock, D.H., Petticrew, E.L., Salomons, W., Trustrum, N.A., 2005. Fine-grained sediment in river systems: Environmental significance and management issues. *River Research & Applications,* **21**, 693-717.

Paquet, E., Gailhard, J., Garçon, R., 2006. Evolution of the GRADEX method : improvement by atmospheric circulation classification and hydrological modelling, *La Houille Blanche,* **5**, 80-90.

Packman, AI., Mackay, JS., 2003. Interplay of stream-subsurface exchange, clay deposition and stream bed evolution. *Water Resources Research,* **39**: 411–419.

Poirel, A., 2004. Etude du transport solide dans la Durance; Résultats des mesures 2001-2003. EDF. Internal technical report, 34 p.

Poulenard, J., Legout, C., Némery, J., Bramoski, J., Navratil, O., Fanget, B., Perrette, Y., Evrard, O., Estèves, M., in press. Tracing sources of sediments during flood events by diffuse reflectance infrared fourier-transform (DRIFT): a case study in highly erosive mountain catchment (Southern French Alps). *Journal of Hydrology*.

Regües D., Gallart, F., 2004. Seasonal patterns of runoff and erosion responses to simulated rainfall in a badland area in Mediterranean mountain conditions (Vallcebre, Southeastern Pyrenees). *Earth Surf. Process. Landforms,* **29:** 755–767. DOI: 10.1002/esp.1067

Rey, F., 2009. A strategy for fine sediment retention with bioengineering works in eroded marly catchments in a mountainous Mediterranean climate (Southern Alps, France). *Land Degradation & Development*, **20**: 210 – 216.

Reyss, J. L., Schmidt, S., Legeleux, F., Bonté, P., 1995. Large, low background well-type detector for measurements of environmental radioactivity. *Nuclear Instruments & Methods,* A357, 391-397.

Salomons, W., Forstner, U., 1984. *Metals in the Hydrocycle*. Springer-Verlag: New York.

Schmidt, K. H., Morche, D., 2006. Sediment output and effective discharge in two small high mountain catchments in the Bavarian Alps, Germany. *Geomorphology*, **80** (1-2), 131-145.

Seeger, M., Errea, M. P., Begueria, S., Arnaez, J., Marti, C., Garcia-Ruiz, J. M., 2004. Catchment soil moisture and rainfall characteristics as determinant factors for discharge/suspended sediment hysteretic loops in a small headwater catchment in the Spanish Pyrenees. *Journal of Hydrology*, **288**: 299–311.

Skalak, K., Pizzuto, J.. 2010. The distribution and residence time of suspended sediment stored within the channel margins of a gravel-bed bedrock river. *Earth Surf. Process. Landforms.* **35**, 435–446.

Smith, H.G., Dragovich, D., 2009. Interpreting sediment delivery processes using suspended sediment-discharge hysteresis patterns from nested upland catchments, south-eastern Australia. *Hydrol. Process.* **23**, 2415–2426.

Tacon, S., Liébault, F., Piégay, H., 2011. LiDAR-derived morphological changes of gravel-bed rivers in the French Prealps. European Geophysical Union Conference EGU2011, **13,** 7165.

884 Walling, DE., Collins, AL., 2008. The catchment sediment budget as a management tool.
885 *Environmental Science and Policy*, **2**: 136–143.
886 Wang, J., Bai, S. B., Liu, P., Li, Y. Y., Gao, Z. R., Qu, G. X., Cao, G. J., 2009. Channel
887 sedimentation and erosion of the Jiangsu reach of the Yangtze River during the last 44
888 years. *Earth Surf. Process. Landforms*, **34**, 1587–1593
889 Williams, G.P., 1989. Sediment concentration versus water discharge during single
890 hydrologic events in rivers. *J. Hydrol.*, **111**, 89-106.
891 Yamakoshi, T., Mathys, N., Klotz N., 2009. Time-lapse video observation of erosion
892 processes on the Black Marls badlands in the Southern Alps, France. *Earth Surf. Process.*
893 *Landforms*, **34**: 314–318
894

895 **Table and Figure captions**

896 Table 1: River monitoring stations and characteristics of their draining areas

897

898 Table 2: Floods investigated in this study (W: widespread; S: storm) and analyses conducted
899 (X: available; n/a: not available).

900

901 Table 3: Concentrations in geochemical elements (mg kg^{-1}) and mean radionuclide activities
902 (in Bq kg^{-1}, except for K – in %) analysed in the representative source material samples
903 sieved to < 63 µm.

904

905 Table 4: Discharge and sediment indicators derived from the river station monitoring between
906 October 2007 and December 2009.

907

908 Table 5: Concentrations in geochemical elements (mg kg^{-1}) and mean radionuclide activities
909 (in Bq kg^{-1}, except for K – in %) analysed in the samples of suspended sediment.

910

911 Figure 1: Location of the study area, rainfall radars, river monitoring stations (STA1–STA5)
912 and raingauges (R1–R15) within the Bléone catchment.

913

914 Figure 2: Geology of the Bléone catchment and location of the river monitoring stations.

915

916 Figure 3: Suspended Sediment Yield (SSY) within the Bléone catchment between 2007 –
917 2009. (a) Inter-annual variability (in % in Figure 3a and in t km^{-2} in associated Table). (b)
918 Fraction of the total SSY attributed to Q–SSC clockwise, anticlockwise and concomitant

floods. (c) Occurrence of Q–SSC clockwise, anticlockwise and concomitant floods at each station and for each rainfall regime (widespread and storm).

Figure 4: Rainfall intensity (mm h^{-1}) vs. rainfall total amount (mm) measured at the raingauges of the Bléone catchment with a 10-minutes time-step (R1 – R10).

Figure 5: Relationship between suspended sediment yield (SSY; t) and peak discharge (Qmx; m^3 s^{-1}) for the floods that occurred in the Bléone catchment between October 2007 and December 2009. Several events were selected for further analysis (see Table 2 for details).

Figure 6: Hydrological regime close to the catchment outlet (STA1) between 2007 and 2009, and timing of the floods selected for further investigation (W1, W2; S1 – S3).

Figure 7: Case study W1: temporal dynamics of the December 22, 2009 flood that occurred on the Bès River at Pérouré (STA4) station (a) Radar rainfall image showing the maximum hourly rainfall depths during the event; (b) Picture of the Bès river reaching a 30 m^3 s^{-1} discharge and taken from the monitoring station, (c) evolution of rainfall (data available from R1 – R2 and R15 gauges; Fig. 1), discharge (Q; red curve) and SSC (black curve) during the flood and timing of sediment sampling (F1–F6); (d) evolution of sediment source contribution (in t per 10 min) in suspended sediment; (e) Q–SSC clockwise hysteretic relationship (and timing of sediment sampling) observed on the Bès River at Pérouré.

Figure 8: Topographical survey of a selected braided reach of the Bès River. (a) Picture of the reach located between Pérouré and Esclangon and taken on 3 March 2009. (b) Topographical survey of cross-section T1 before (18 April 2009) and after (3 March 2010) the 22 December

944 2009 flood. (c) Aerial pictures of the reach taken in 2004 and 2010 with the delineation of the
945 alluvial margins (dashed lines) and the main channel (plain line) before the 22 December
946 2009 flood.
947
948 Figure 9: Case study W2: temporal dynamics of the succession of floods that occurred
949 between 31 October 2008 and 12 November 2008 on the Galabre River at Robine (STA2). (a)
950 Evolution of rainfall (P; R3 raingauge), discharge (Q; red curve) and SSC (black curve)
951 during the flood and timing of sediment sampling (B1– B3); (b) Evolution of sediment source
952 contributions to suspended sediment (pie-charts); (c) radar images showing the maximum
953 hourly rainfall depths during the events; (d) Q–SSC hysteretic relationship (and timing of
954 sediment sampling).
955
956 Figure 10: Case study S1: temporal dynamics of the flood that occurred on 12 August 2008 on
957 the Galabre River at Robine (STA2). (a) Radar images showing the maximum hourly rainfall
958 depths during the event; (b) Evolution of rainfall (P; R3 raingauge), discharge (Q; red curve)
959 and SSC (black curve) during the flood and timing of sediment sampling (A1–A5); (c) Q–
960 SSC hysteresis relationship (and timing of sediment sampling); (d) evolution of sediment
961 source contributions to suspended sediment.
962
963 Figure 11: Case study S2: temporal dynamics of the 30 June 2009 flood that propagated
964 across the entire Bléone catchment (STA1, 2, 4 and 5). (a) Spatial distribution of maximum
965 hourly rainfall; (b) comparison of rainfall data provided by 4 different rain gauges; (c) This
966 picture of the Bléone River at the Prads station was taken at 14:38 GMT. (d) Discharge and
967 SSC measured at the different stations (corresponding to red and black curves, respectively);
968 pie-charts indicate the sources of suspended sediment.

Figure 12: Case study S3: temporal dynamics of the 7 August 2009 flood that occurred on the Bès River at Pérouré (STA4) and Esclangon (STA3) stations. (a) Radar rainfall image showing the maximum hourly rainfall depths during the event; (b) evolution of rainfall during the event (as recorded by R1-R2-R3-R14 rain gauges), (c) evolution of discharge (Q; red curve) and SSC (Pérouré: black curve; Eclangon: grey curve) during the flood and timing of sediment sampling (D1–D6); (d) evolution of sediment source contributions to suspended sediment (pie-charts); (e) Q–SSC anti-clockwise hysteresis relationship (and timing of sediment sampling) observed on the Bès river at Pérouré.

Figure 13: Proportion of draining catchment surface occupied by the different lithologic sources (%, black bars), riverbed sediment composition (%; white bars; Evrard et al., 2011) and suspended sediment composition (grey bars; mean ± min./max. range of values obtained for the entire series of samples collected; this study) at the different river monitoring stations in the Bléone catchment.

Table 1: River monitoring stations and characteristics of their draining areas

Station Number	River	Location	Drainage Area (km²)	Highly Eroded Area (%)	Geology (% area) [1]				Land use (% area) [2]					Sampling frequency	
					Quaternary deposits	Conglomerate	Limestones / marls	Black marls	Forest	Cropland	Bare rocks	Sparse vegetation	Grassland	Water Level	Turbidity
STA1	Bléone	Le Chaffaut	713	11	27	25	37	10	43.6	5.0	6.9	30.7	13.1	Variable time-step	60 min.
STA2	Galabre	La Robine	22	8	31	2	54	9	11.0	2.6	0.0	19.3	67.0	10 min.	10 min.
SAT3	Bès	Esclangon	181	17	20	15	51	12	42.6	1.9	15.7	18.2	21.4	n/a[3]	10 min.
STA4	Bès	Pérouré	165	17	20	15	51	12	42.6	1.9	15.7	18.2	21.4	Variable	10 min.
STA5	Bléone	Prads	65	7	37	15	46	2	24.2	0.0	33.9	33.9	6.3	10 min.	10 min.

[1] The remaining % correspond to gypsum

[2] The remaining % correspond to urban areas

[3] n/a: no data available

Table 2: Floods investigated in this study (W: widespread; S: storm) and analyses conducted (X: available; n/a: not available).

Event Date	Case study code	Samples	Hail	Snow Cover	Rainfall			Analysis			
					Duration (hr)	Volume (mm)	Intensity [1] (mm h^{-1})	River monitoring	Rainfall	Sediment fingerprinting	Topography and imagery
22/12/2009	W1	F1 – F6	no	yes	21	108[4]	20	X	X	X	X
31/10/2008	W2a	B1	no	no	16	67[3]	9	X	X	X	n/a
02/11/2008	W2b	B2	no	no	49	33[3]	15	X	X	X	n/a
12/11/2008	W2c	B3	no	no	16	77[3]	19	X	X	X	n/a
12/08/2008	S1	A1 – A5	no	no	4	24[3]	90	X	X	X	n/a
29/06/2009	S2	C1 – C6	yes	no	5	6[2]	30	X	X	X	n/a
07/08/2009	S3	D1 – D6	no	no	5	61[2]	63	X	X	X	n/a

[1] Maximum intensity derived from 10-minutes time-step rainfall data, except for W3 and W4 case studies
[2] Estimated based on data from the Haut-Vernet raingauge
[3] Estimated based on data from the Ainac raingauge
[4] Estimated based on data from the Barles raingauge
[5] Estimated based on data from the Laval raingauge (Draix Observatory)

Table 3: Concentrations in geochemical elements (mg kg^{-1}) and mean radionuclide activities (in Bq kg^{-1}, except for K – in %) analysed in the representative source material samples sieved to < 63 µm.

Source type		Mg	Al	Ca	Ti	V	Mn	Ni	Cu	Ag	Cd	Sb	Ba	Tl	Pb	Pb-210	K (%)	Cs-137	Th-234	Ra-226	Ra-228	Th-228
Black marl (Bathonian) -	mean	9276	77328	148962	464	125	844	48	21	0.20	0.17	0.39	216	0.55	14	32	1.7	12	26	21	32	33
	SD	2816	10535	74803	810	28	132	9	9	0.04	0.04	0.10	24	0.10	5	19	0.4	26	6	3	7	7
Other black marls -	mean	8661	61733	127430	4272	90	549	41	20	0.17	0.18	0.41	248	0.47	16	39	1.6	26	26	22	33	32
	SD	3231	20399	57737	1118	26	121	8	6	0.03	0.05	0.07	87	0.12	5	14	0.5	24	7	5	11	11
Grey marls-	mean	41086	55698	134353	3565	88	634	43	18	0.18	0.20	0.77	192	0.35	12	62	1.5	71	28	25	28	28
	SD	64278	6261	104767	1084	12	404	4	3	0.06	0.09	0.54	49	0.05	3	43	0.5	121	11	8	8	8
Marly limestones-	mean	24744	49422	97944	3197	78	444	47	19	0.18	0.25	0.76	216	0.49	12	52	1.8	23	40	42	24	25
	SD	27485	1583	82709	207	17	38	21	11	0.08	0.14	0.35	78	0.22	5	1	0.9	4	4	2	2	1
Quarternary deposits-	mean	11355	41394	205027	3398	50	198	24	10	0.14	0.16	0.68	171	0.37	11	42	1.0	44	33	32	41	40
	SD	1307	355	11074	138	1	20	1	1	0.00	0.01	0.09	2	0.00	1	2	0.1	57	0	1	1	0
Conglomerates-	SD	10340	87905	162631	3480	86	658	60	32	0.29	0.38	0.74	397	0.49	24	51	1.4	40	24	20	33	33
	SD	2438	7914	22337	146	16	105	17	1	0.08	0.03	0.03	43	0.09	6	19	0.2	22	2	1	2	5

n/a: not available

To facilitate their analysis and interpretation, the six rock types were regrouped into five classes (black marls of Bathonian age and other black marls were regrouped in one class; grey marls and marly limestones were regrouped in one class entitled “limestones”).

Table 4: Discharge and sediment indicators derived from the river station monitoring between October 2007 and December 2009.

Station Number	Station Name	Number of events	Q_m (mm)	Q_{mx} (m^3s^{-1})	SSC_m (g l^{-1})	SSC_{mx} (g l^{-1})	SSY (t)	SSY* (t km^{-2} yr^{-1})	Ms2 (%)	V2 (%)	SSYw (%)
STA1	Bléone at Chaffaut	83	410	500	0.28	46	641,900 ± 192,600	330 ± 100	75	18	82
STA4	Bes at Pérouré	89	437	170	0.30	135	256,300 ± 76,900	690 ± 207	96	16	89
STA5	Bléone at Prads	55	572	18	0.12	360	66,200 ± 19,900	452 ± 136	99.9	12	72
STA2	Galabre at Robine	75	400	34	0.42	130	33,500 ± 10,000	680 ± 200	96	20	80

Discharge parameters: Q_m (mean annual runoff depth); Q_{mx} (instantaneous peak flow discharge); sediment concentration parameters: SSC_m (mean sediment concentration); SSC_{mx} (peak sediment concentration); sediment yield parameters: *SSY* (total sediment yield); *SSY** (specific sediment yield); Ms2% and V2%, respectively the percentage of total mass of suspended solid and water volume transported during 2% of the observational period; SSYw, the fraction of inter-annual sediment yields transported during widespread rainfall events; (1-SSYw) is the SSY transported during storms.

Table 5: Concentrations in geochemical elements (mg kg^{-1}) and mean radionuclide activities (in Bq kg^{-1}, except for K – in %) analysed in the samples of suspended sediment.

Sample	Date	Time	Site	SSC (g l^{-1})	Mg	Al	Ca	Ti	V	Mn	Ni	Cu	Ag	Cd	Sb	Ba	Tl	Pb	excess-Pb-210	K (%)	Cs-137	Th-234	Ra-226	Ra-228	Th-228	Be-7
Case S1: Summer storm on the Galabre river at Robine (STA2)																										
A1	12/08/2008	20:00	Robine	69	9260	60567	152613	5074	122	495	48	19	0.13	0.10	0.54	303	0.56	16.0	31.8	2.0	11.1	0.0	33.0	27.1	3.3	n/a
A2	12/08/2008	21:00	Robine	5	93184	643623	960926	1986	90	369	19	15	0.05	0.10	0.13	124	0.26	6.0	59.2	2.1	17.5	19.5	4.5	22.0	0.9	n/a
A3	12/08/2008	23:20	Robine	60	14075	65480	164390	3367	83	406	37	12	0.11	1.23	0.35	172	0.49	23.9	15.3	1.8	3.6	23.9	3.8	21.5	0.7	n/a
A4	13/08/2008	00:20	Robine	133	12593	70991	213958	2763	69	279	29	9	0.09	0.56	0.27	145	0.41	13.8	14.1	1.5	4.2	27.5	3.7	22.5	0.7	n/a
A5	13/08/2008	07:20	Robine	38	8881	61401	157484	3134	87	229	29	9	0.12	0.24	0.36	182	0.55	11.9	17.9	1.7	4.7	0.0	33.0	27.1	3.3	n/a
Case W2: Widespread flood on the Galabre river at Robine (STA2)																										
B1	31/10/2008	12:30	Robine	8	10894	47052	204417	3663	103	526	42	18	0.13	0.11	0.66	198	0.45	13.5	14.9	1.7	3.6	21.2	3.5	22.6	0.7	n/a
B2	02/11/2008	21:30	Robine	26	12841	44731	203326	3525	101	575	42	19	0.12	0.14	0.63	198	0.45	15.3	0.0	1.8	3.0	27.8	3.7	23.2	0.7	n/a
B3	12/11/2008	02:20	Robine	25	16681	48372	176958	3804	111	675	39	23	0.14	0.12	0.70	212	0.54	19.5	10.4	2.0	4.4	29.9	2.5	25.2	0.5	n/a
Case S2: Storm propagation from Prads (STA5) to Chaffaut (STA1)																										
C1	29/06/2009	16:40	Robine	21	10297	79426	99000	4725	97	349	42	15	0.14	0.19	0.37	289	0.62	11.8	12.4	2.1	5.8	36.4	3.8	26.6	0.7	n/a
C2	29/06/2009	23:40	Robine	27	18741	107071	105745	4238	118	617	50	16	0.14	0.29	0.43	218	0.69	14.9	15.6	2.5	4.6	29.9	4.1	22.8	0.7	n/a
C3	29/06/2009	14:30	Prads	61	9431	80880	191885	3313	96	294	50	39	0.29	0.48	0.46	598	0.64	16.4	36.3	1.8	17.8	31.4	3.3	27.0	0.6	n/a
C4	30/06/2009	01:10	Pérouré	7	12484	104465	106063	5798	128	870	46	20	0.17	0.41	0.79	227	0.81	15.2	38.7	2.6	5.8	33.0	2.3	27.8	0.4	n/a
C5	29/06/2009	23:00	Le Chaffaut	10	7475	68408	143835	3296	100	327	49	37	0.24	1.28	0.52	615	0.70	28.4	75.7	1.8	22.2	37.0	5.4	35.0	1.1	n/a
C6	30/06/2009	05:30	Le Chaffaut	1	10361	88608	160721	4664	160	558	73	58	0.38	0.69	2.43	973	1.08	22.8	58.0	2.0	20.5	0.0	54.8	28.2	5.6	n/a
Case S3: Summer storm on the Bès river between Pérouré(STA4) and Esclangon (STA3)																										
D1	07/08/2009	17:50	Pérouré	11	11103	60185	227286	3488	84	642	45	22	0.15	0.28	0.35	220	0.45	12.5	14.2	1.3	2.3	13.2	19.2	25.9	28.3	n/a
D2	07/08/2009	19:50	Pérouré	157	8783	78061	129692	4204	118	1128	51	22	0.18	0.23	0.55	265	0.65	13.3	21.8	1.8	2.0	30.3	24.8	40.7	37.0	n/a
D3	07/08/2009	22:50	Pérouré	46	7868	72041	127575	3552	103	796	44	21	0.16	0.14	0.29	278	0.58	10.4	14.9	1.9	4.5	22.6	23.5	39.0	36.6	n/a
D4	07/08/2009	18:50	Esclangon	10	8567	44512	208399	2693	62	468	35	15	0.10	0.15	0.28	150	0.34	8.7	0.0	1.3	4.0	13.8	18.4	21.9	25.9	n/a
D5	07/08/2009	21:50	Esclangon	128	8904	81752	132215	4463	130	1186	58	23	0.24	0.16	0.65	311	0.76	13.9	0.0	2.0	2.6	26.1	23.5	34.6	39.5	n/a
D6	08/08/2009	01:50	Esclangon	33	8585	85098	135913	4190	126	869	51	24	0.23	0.28	0.59	263	0.71	13.2	31.2	2.0	5.5	30.1	22.2	38.8	38.8	n/a
Case W1: Widespread flood on the Bès river at Pérouré (STA4)																										
F1	22/12/2009	16:00 - 18:00	Pérouré	1 - 4	12136	73591	157582	3667	96	546	47	19	0.15	0.17	0.63	178	0.53	11.6	0.0	1.8	2.9	24.3	6.6	21.8	1.2	33
F2	22/12/2009	20:00	Pérouré	21	12052	63125	183479	2999	78	514	42	18	0.15	0.15	0.35	152	0.42	11.2	11.3	1.4	3.4	29.5	3.7	20.3	0.7	41
F3	22/12/2009	22:00	Pérouré	28	12309	50620	202141	2645	69	580	39	18	0.11	0.24	0.45	164	0.45	14.6	11.0	1.4	5.2	21.3	4.5	25.9	0.9	<1
F4	23/12/2009	00:00	Pérouré	28	13428	54016	194205	2783	72	641	40	16	0.12	0.21	0.46	178	0.48	11.2	9.3	1.6	6.9	20.2	4.3	25.4	0.9	<1
F5	23/12/2009	03:00	Pérouré	14	10943	45461	173693	2860	74	720	42	19	0.13	0.19	0.52	210	0.47	12.2	14.8	1.4	5.1	25.9	4.2	22.8	0.8	18
F6	23/12/2009	10:00 - 13:00	Pérouré	1 - 3	13533	58182	230516	2782	78	671	42	20	0.13	0.24	0.65	206	0.49	12.1	0.0	1.6	2.9	20.1	5.7	27.0	1.2	<1

n/a: not available

Figure 1: Location of the study area and rainfall radars (Fig. a), river monitoring stations (STA1–STA5) and raingauges (R1–R15) within the Bléone catchment (Fig. b).

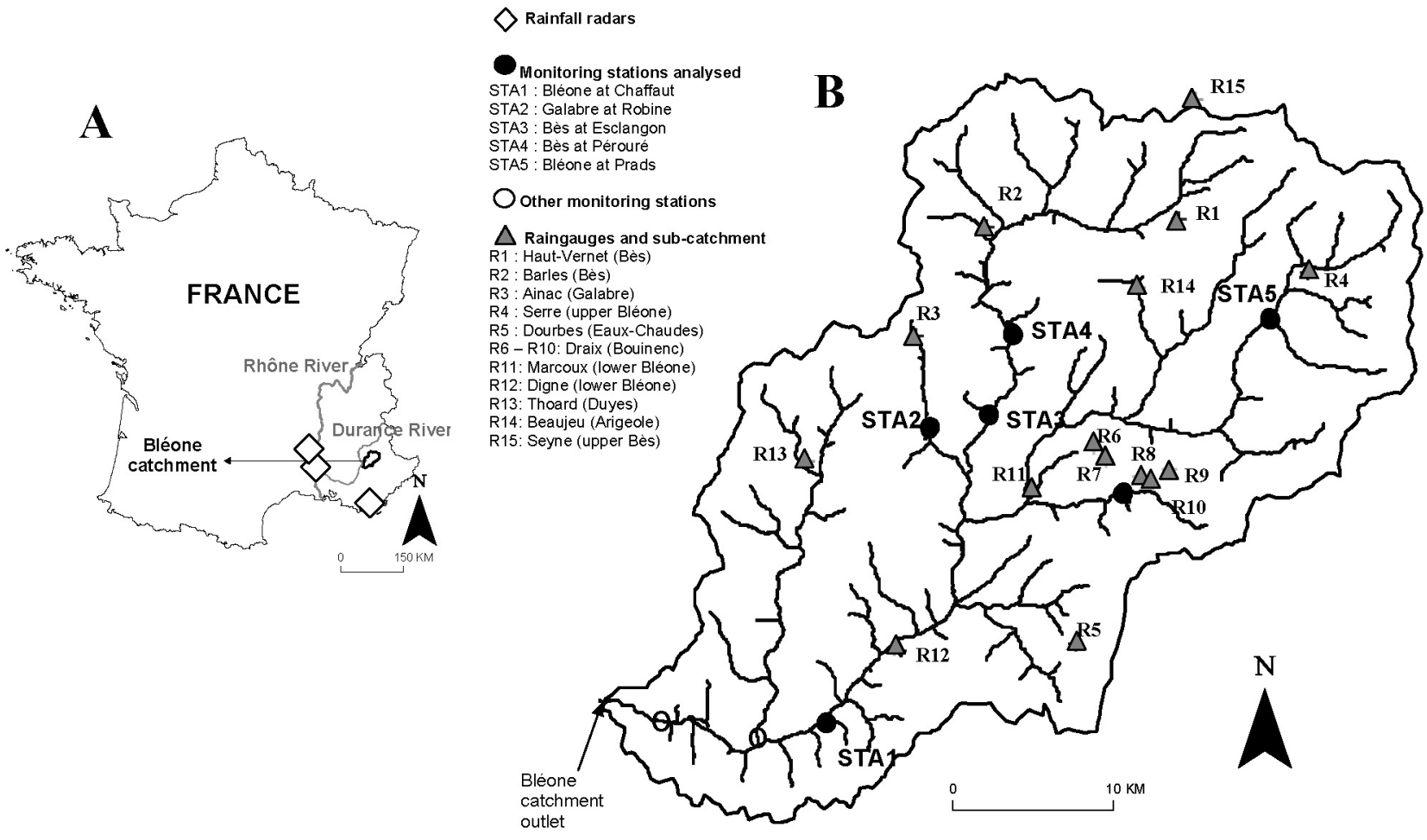

Figure 2: Geology of the Bléone catchment and location of the river monitoring stations

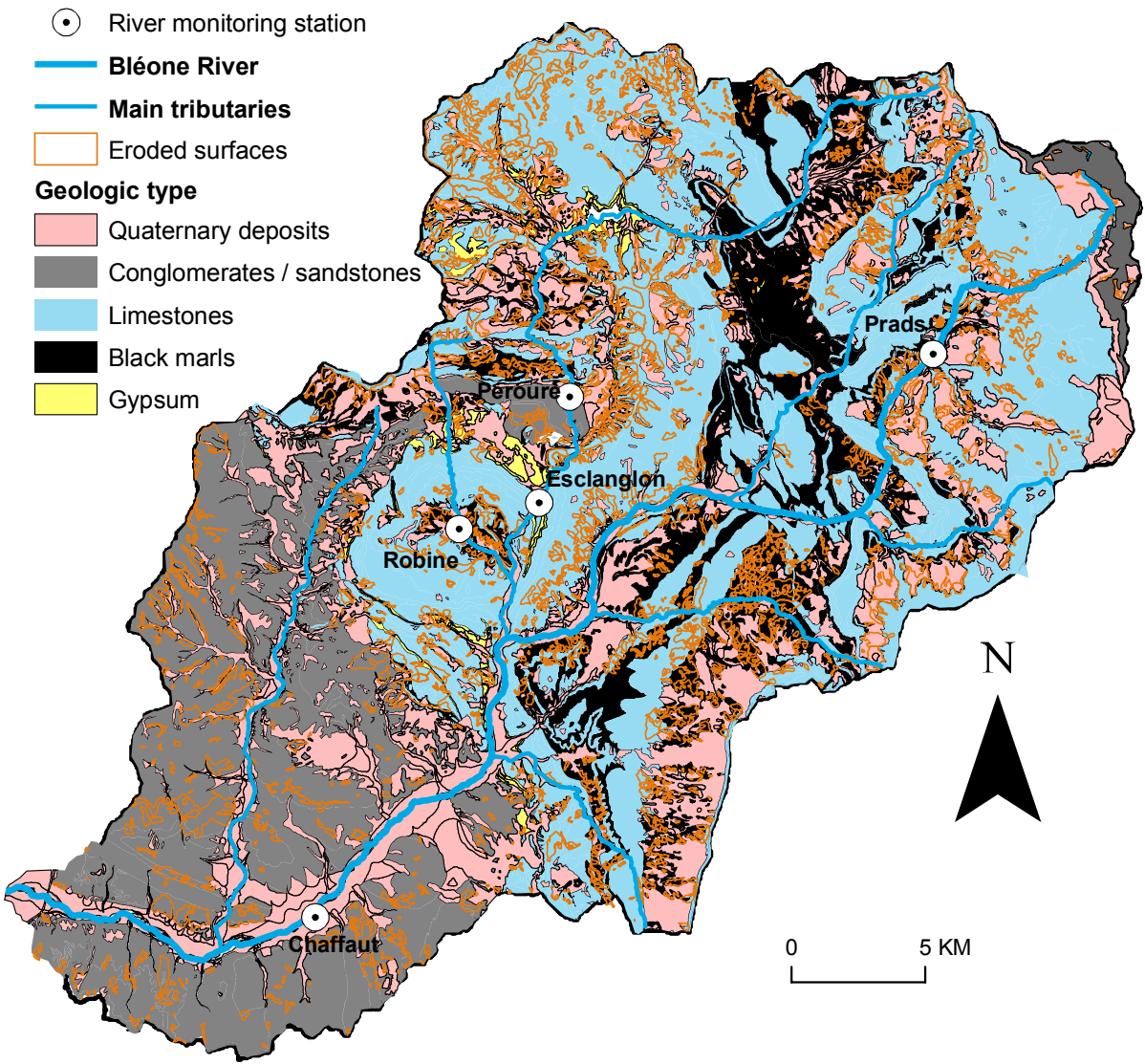

Figure 3: Suspended Sediment Yield (SSY) within the Bléone catchment between 2007 – 2009. (a) Inter-annual variability (in % in Figure 3a and in t km^{-2} in associated Table). (b) Fraction of the total SSY attributed to Q–SSC clockwise, anticlockwise and concomitant floods. (c) Occurrence of Q–SSC clockwise, anticlockwise and concomitant floods at each station and for each rainfall regime (widespread and storm).

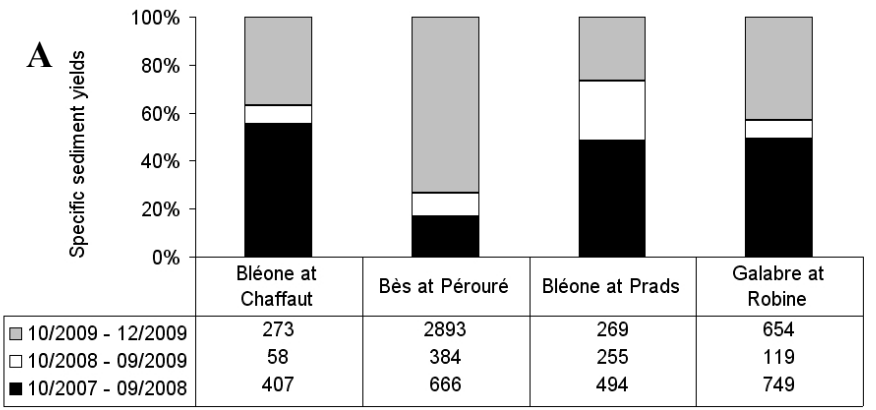

	Bléone at Chaffaut	Bès at Pérouré	Bléone at Prads	Galabre at Robine
10/2009 - 12/2009	273	2893	269	654
10/2008 - 09/2009	58	384	255	119
10/2007 - 09/2008	407	666	494	749

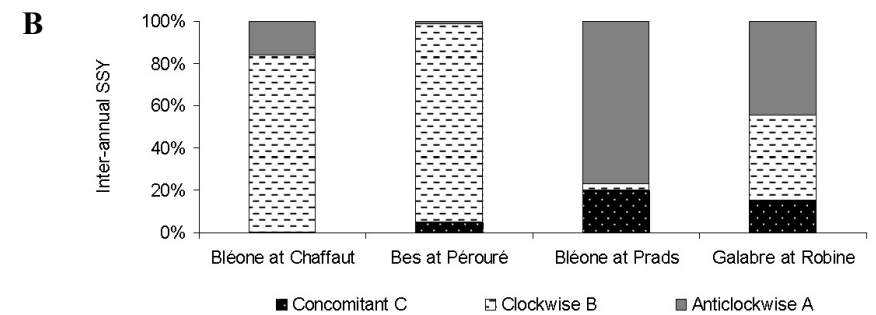

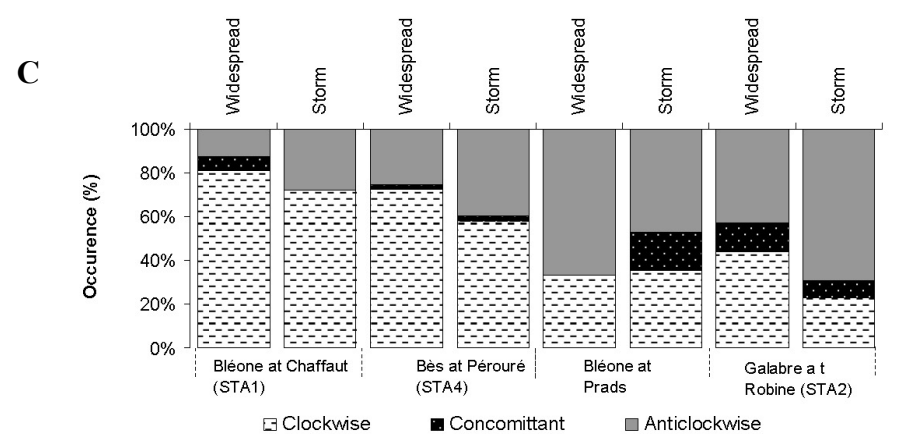

Figure 4: Rainfall intensity (mm h^{-1}) vs. rainfall total amount (mm) measured at the raingauges of the Bléone catchment with a 10-minutes time-step (R1 – R10).

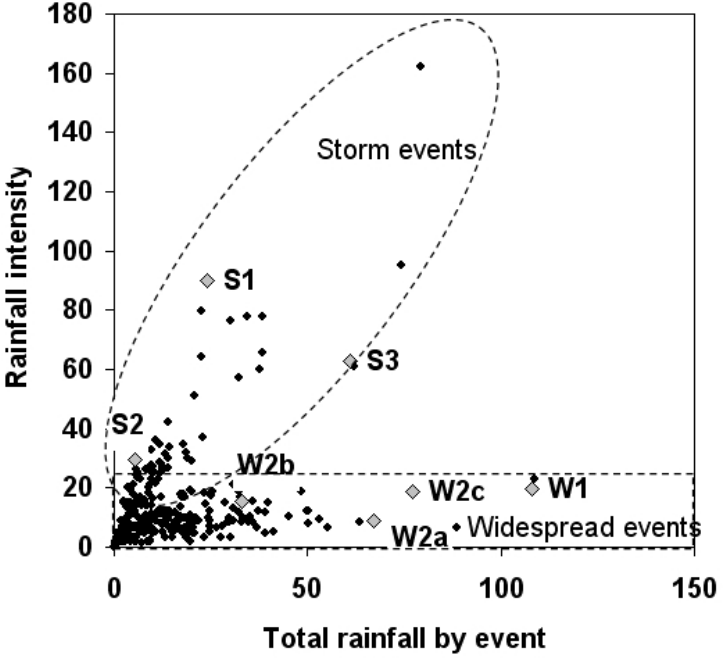

Figure 5: Relationship between suspended sediment yield (SSY; t) and peak discharge (Qmx; m^3 s^{-1}) for the floods that occurred in the Bléone catchment between October 2007 and December 2009. Several events were selected for further analysis (see Table 2 for details).

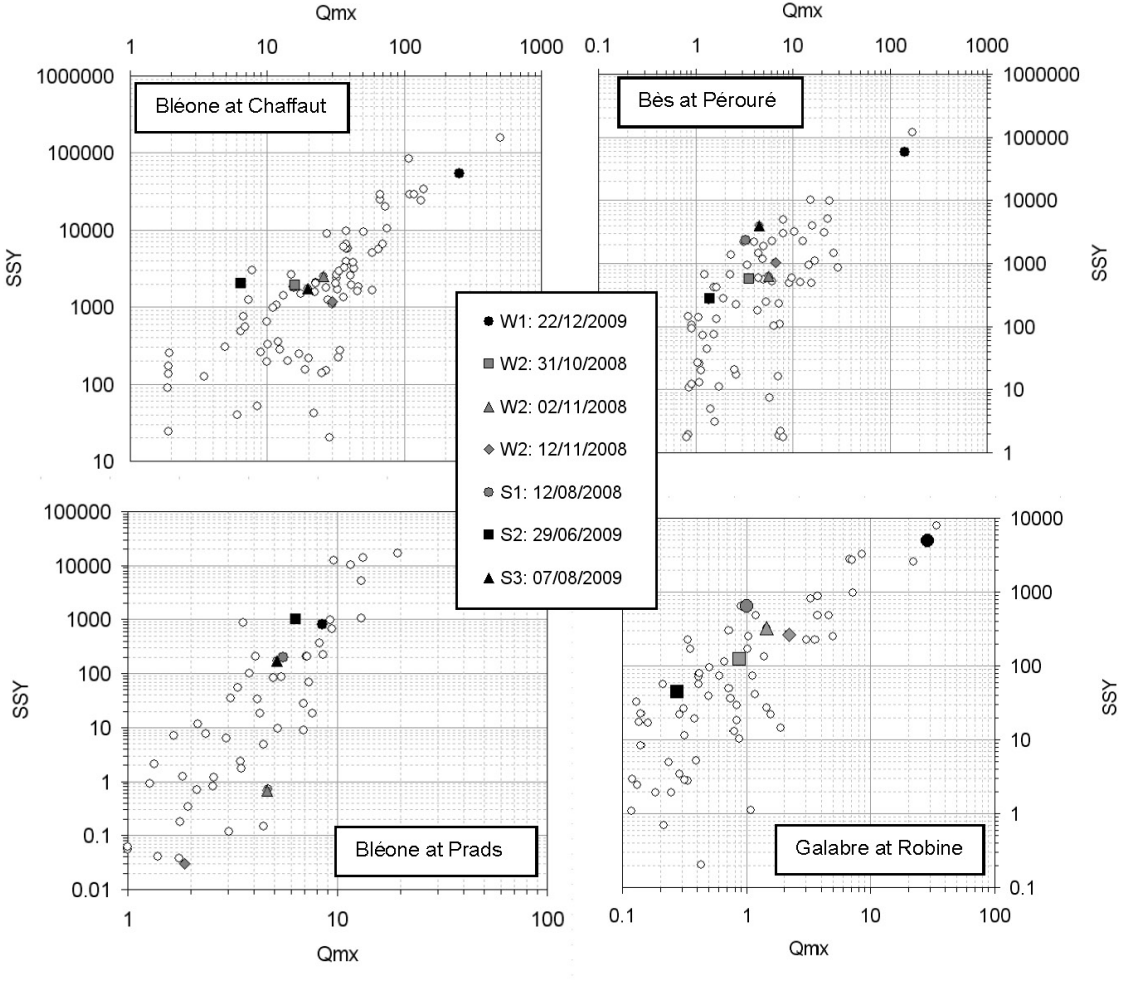

Figure 6: Hydrological regime close to the catchment outlet (STA1) between 2007 and 2009, and timing of the floods selected for further investigation (W1, W2; S1 – S3).

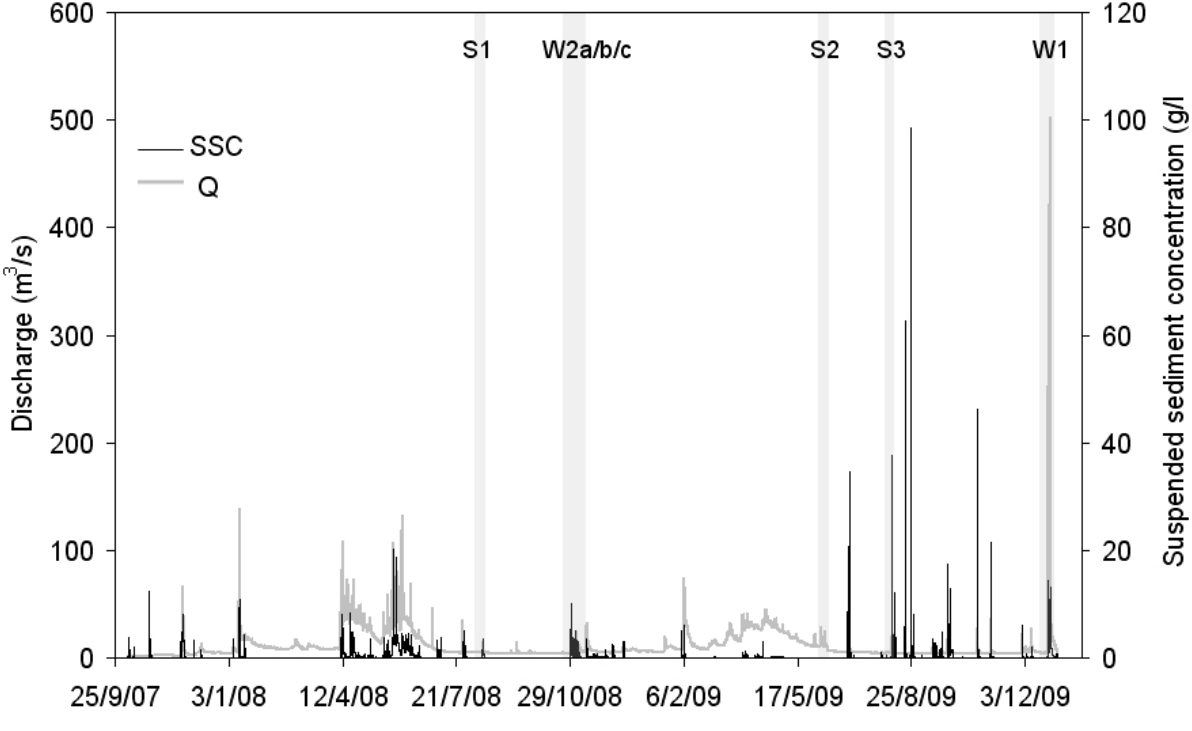

Figure 7: Case study W1: temporal dynamics of the December 22, 2009 flood that occurred on the Bès River at Pérouré (STA4) station (a) Radar rainfall image showing the maximum hourly rainfall depths during the event; (b) Picture of the Bès river reaching a 30 m^3 s^{-1} discharge and taken from the monitoring station, (c) evolution of rainfall (data available from R1 – R2 and R15 gauges; Fig. 1), discharge (Q; red curve) and SSC (black curve) during the flood and timing of sediment sampling (F1–F6); (d) evolution of sediment source contribution (in t per 10 min) in suspended sediment; (e) Q–SSC clockwise hysteretic relationship (and timing of sediment sampling) observed on the Bès River at Pérouré.

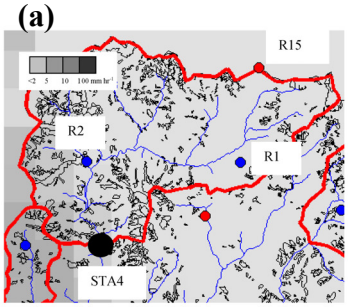

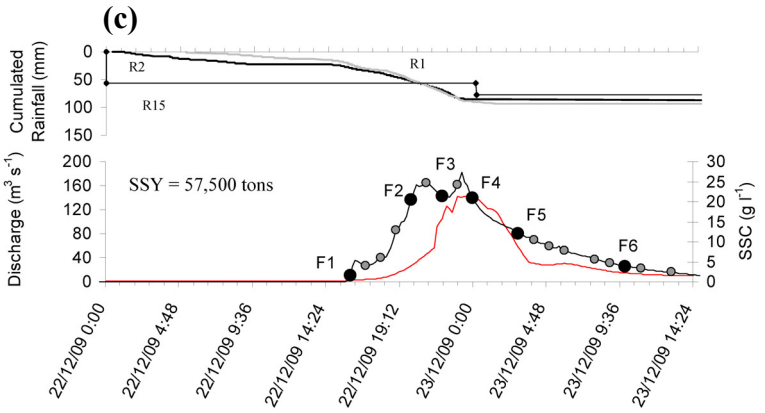

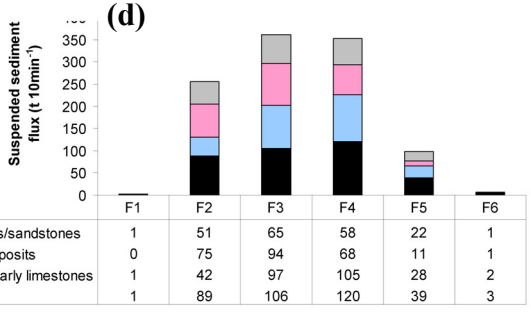

	F1	F2	F3	F4	F5	F6
Conglomerates/sandstones	1	51	65	58	22	1
Quaternary deposits	0	75	94	68	11	1
Limestones/ marly limestones	1	42	97	105	28	2
Black marls	1	89	106	120	39	3

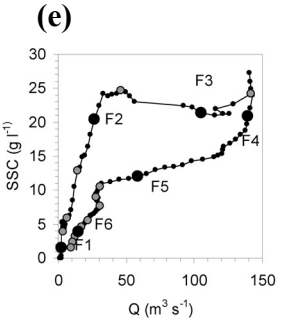

Figure 8: Topographical survey of a selected braided reach of the Bès River. (a) Picture of the reach located between Pérouré and Esclangon and taken on 3 March 2009. (b) Topographical survey of cross-section T1 before (18 April 2009) and after (3 March 2010) the 22 December 2009 flood. (c) Aerial pictures of the reach taken in 2004 and 2010 with the delineation of the alluvial margins (dashed lines) and the main channel (plain line) before the 22 December 2009 flood.

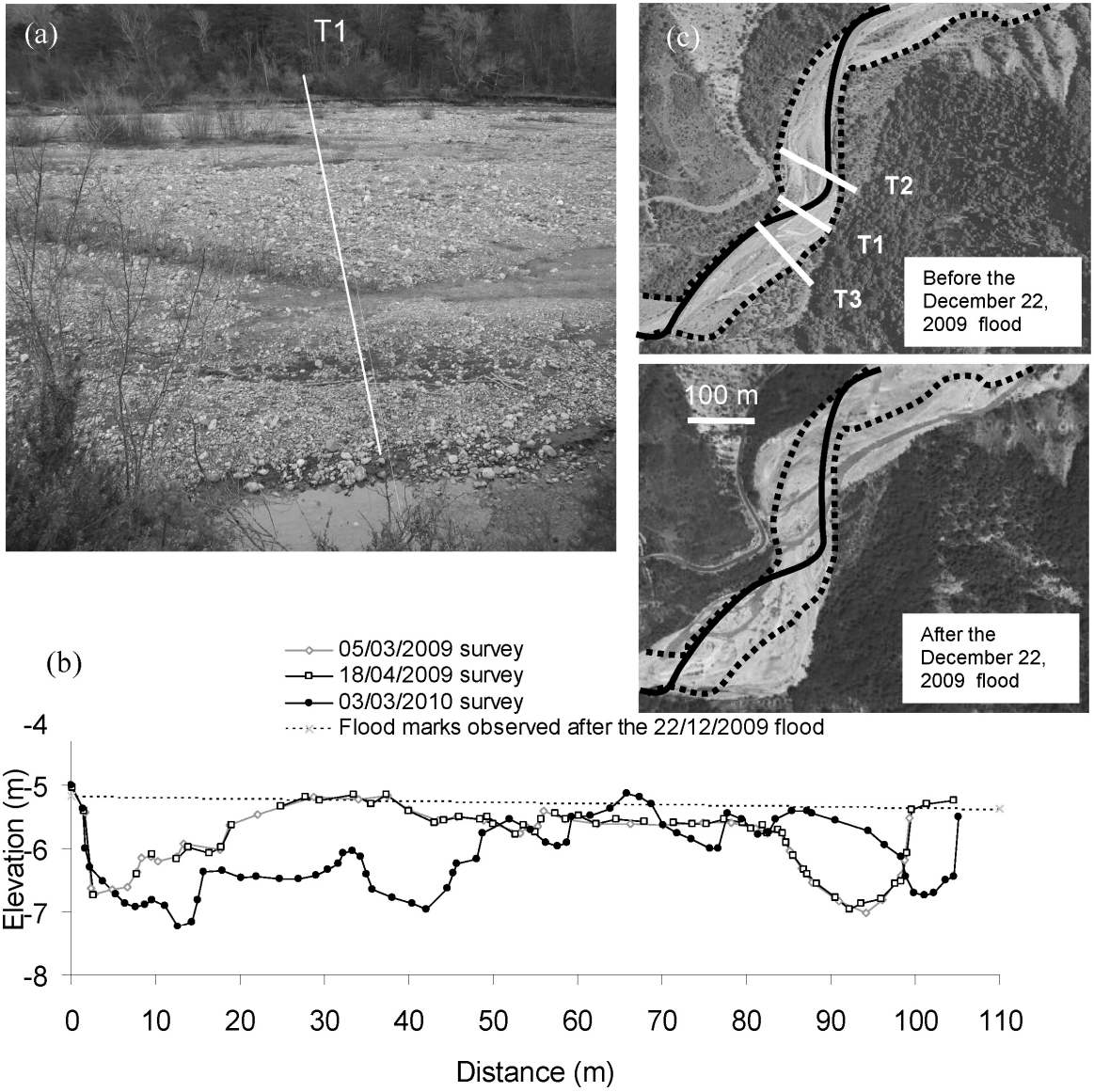

Figure 9: Case study W2: temporal dynamics of the succession of floods that occurred between 31 October 2008 and 12 November 2008 on the Galabre River at Robine (STA2). (a) Evolution of rainfall (P; R3 raingauge), discharge (Q; red curve) and SSC (black curve) during the flood and timing of sediment sampling (B1– B3); (b) Evolution of sediment source contributions to suspended sediment (pie-charts); (c) radar images showing the maximum hourly rainfall depths during the events; (d) Q–SSC hysteretic relationship (and timing of sediment sampling).

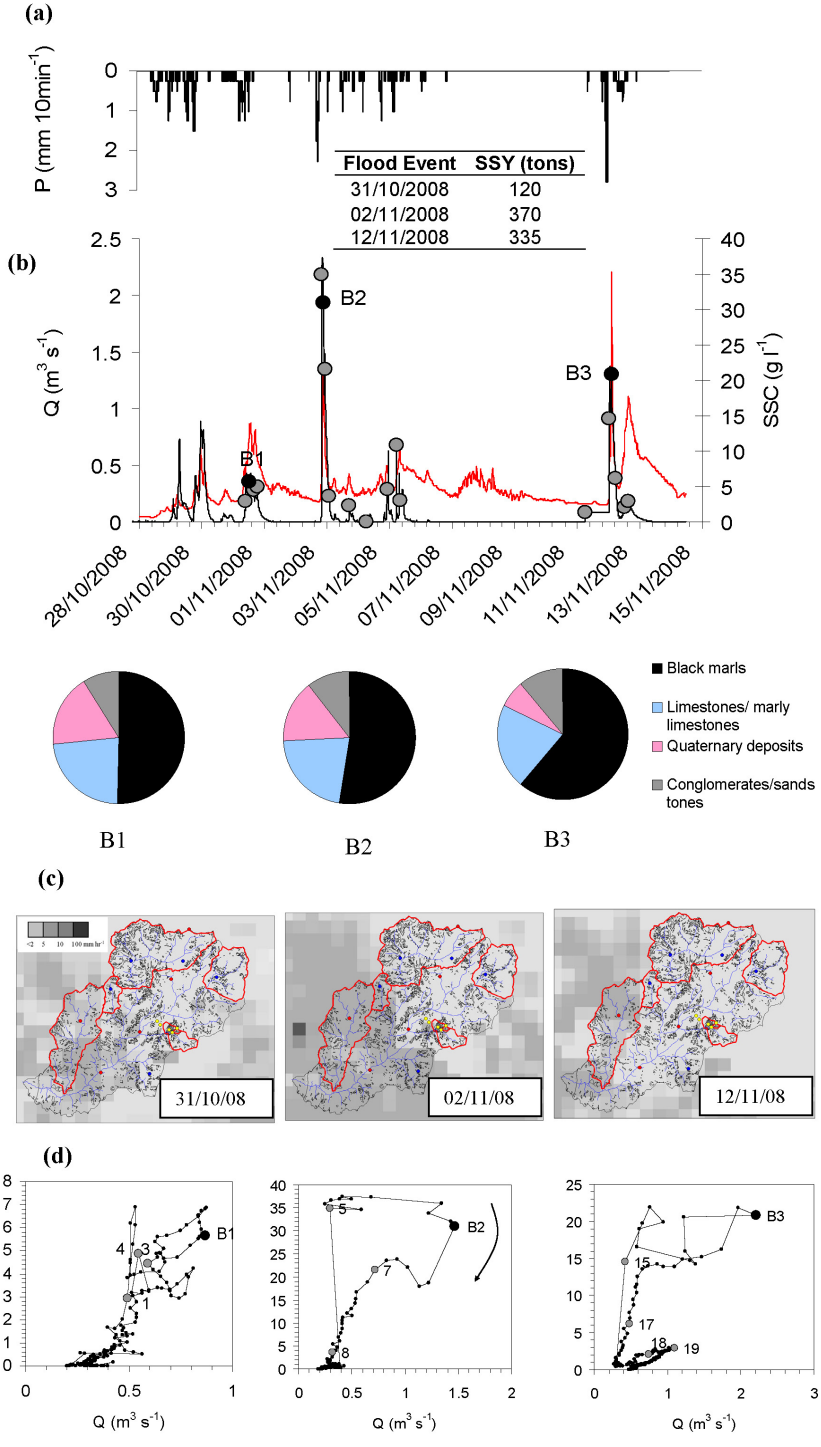

Figure 10: Case study S1: temporal dynamics of the flood that occurred on 12 August 2008 on the Galabre River at Robine (STA2). (a) Radar images showing the maximum hourly rainfall depths during the event; (b) Evolution of rainfall (P; R3 raingauge), discharge (Q; red curve) and SSC (black curve) during the flood and timing of sediment sampling (A1–A5); (c) Q–SSC hysteresis relationship (and timing of sediment sampling); (d) evolution of sediment source contributions to suspended sediment.

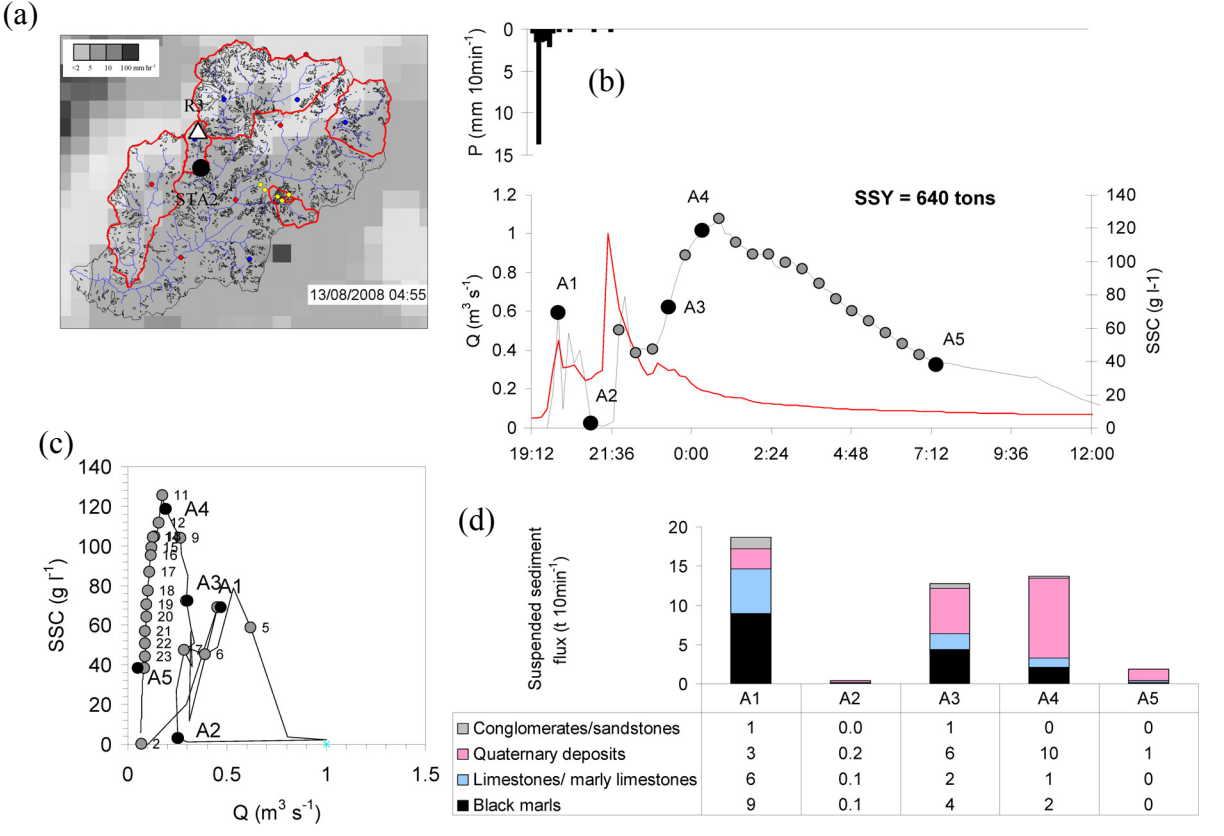

Figure 11: Case study S2: temporal dynamics of the 30 June 2009 flood that propagated across the entire Bléone catchment (STA1, 2, 4 and 5). (a) Spatial distribution of maximum hourly rainfall; (b) comparison of rainfall data provided by 4 different rain gauges; (c) This picture of the Bléone River at the Prads station was taken at 14:38 GMT. (d) Discharge and SSC measured at the different stations (corresponding to red and black curves, respectively); pie-charts indicate the sources of suspended sediment.

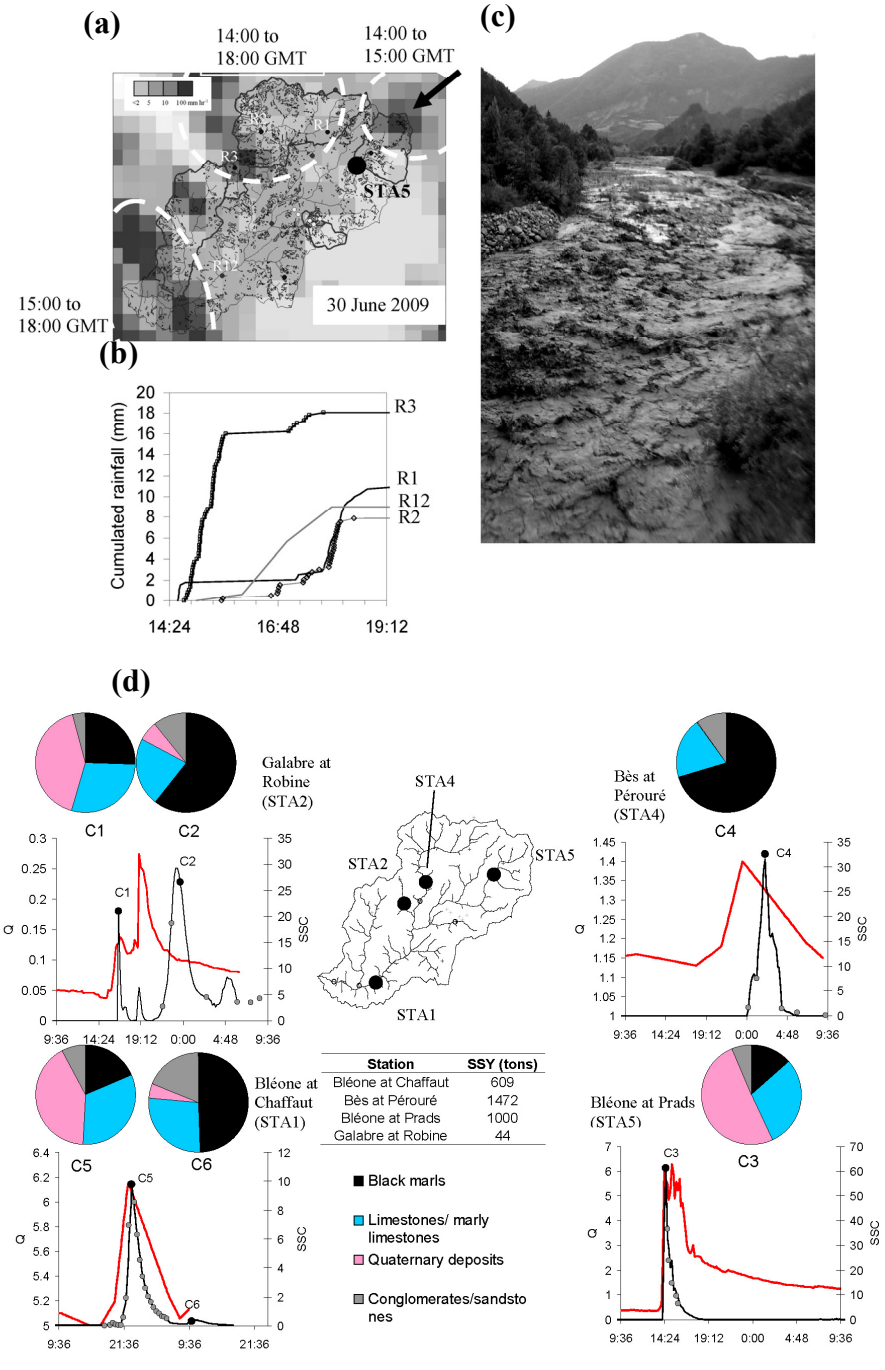

Figure 12: Case study S3: temporal dynamics of the 7 August 2009 flood that occurred on the Bès River at Pérouré (STA4) and Esclangon (STA3) stations. (a) Radar rainfall image showing the maximum hourly rainfall depths during the event; (b) evolution of rainfall during the event (as recorded by R1-R2-R3-R14 rain gauges), (c) evolution of discharge (Q; red curve) and SSC (Pérouré: black curve; Esclangon: grey curve) during the flood and timing of sediment sampling (D1–D6); (d) evolution of sediment source contributions to suspended sediment (pie-charts); (e) Q–SSC anti-clockwise hysteresis relationship (and timing of sediment sampling) observed on the Bès river at Pérouré.

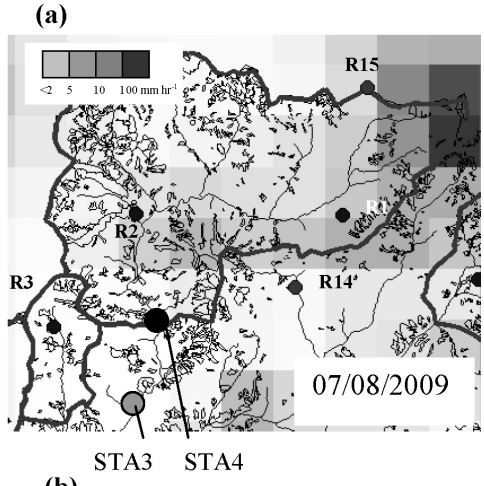

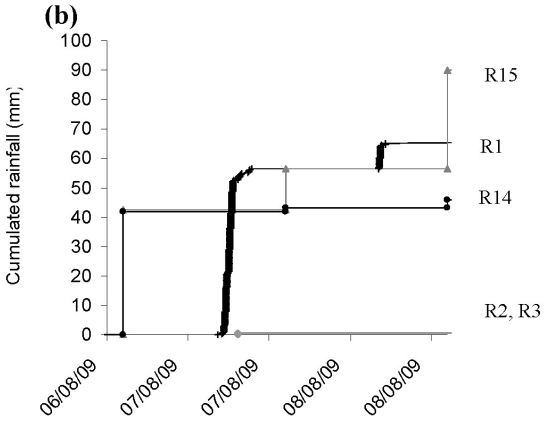

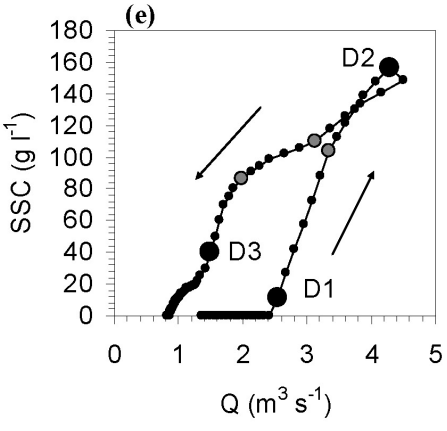

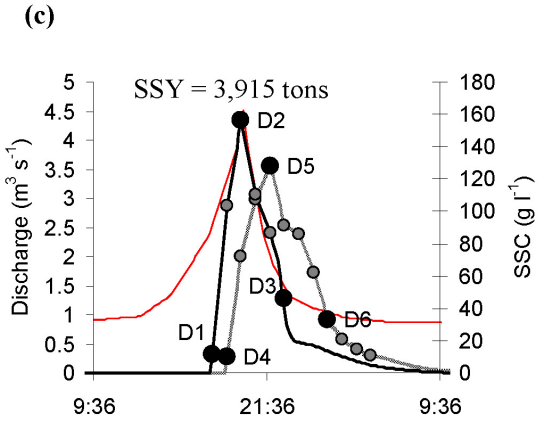

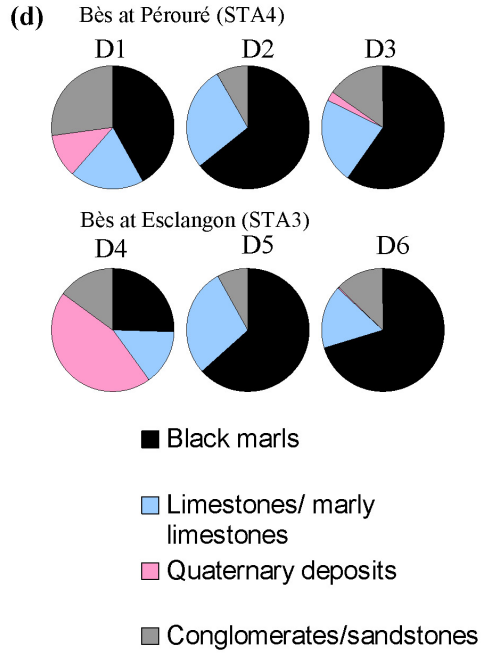

Figure 13: Proportion of draining catchment surface occupied by the different lithologic sources (%, black bars), riverbed sediment composition (%; white bars; Evrard et al., 2011) and suspended sediment composition (grey bars; mean ± min./max. range of values obtained for the entire series of samples collected; this study) at the different river monitoring stations in the Bléone catchment.